2014

Study Of Pd-Ag Membranes With An Intermediate Oxide Layer Fabricated By Surfactant Induced Electroless Plating (Siep)

Md. Moniruddin
North Carolina Agricultural and Technical State University

Study of Pd-Ag Membranes with an Intermediate Oxide Layer Fabricated by Surfactant Induced Electroless Plating (SIEP)

Md. Moniruddin

North Carolina A&T State University

A thesis submitted to the graduate faculty

in partial fulfillment of the requirements for the degree of

MASTER OF SCIENCE

Department: Chemical, Biological and Bioengineering

Major: Chemical Engineering

Major Professor: Dr. Shamsuddin Ilias

Greensboro, North Carolina

2014

The Graduate School
North Carolina Agricultural and Technical State University
This is to certify that the Master's Thesis of

Md. Moniruddin

has met the thesis requirements of
North Carolina Agricultural and Technical State University

Greensboro, North Carolina
2014

Approved by:

Dr. Shamsuddin Ilias Major Professor	Dr. Vinayak N Kabadi Committee Member
Dr. Jianzhong Lou Committee Member	Dr. Stephen B Knisley Department Chair

Dr. Sanjiv Sarin
Dean, The Graduate School

Biographical Sketch

Md. Moniruddin was born on June 10, 1985, in Narsingdi, Bangladesh. He earned his Bachelor of Science degree in Chemical Engineering in 2009 from Bangladesh University of Engineering and Technology (BUET). In 2009, he joined Unilever Bangladesh Limited (Consumer Product Company) as a Production Shift Officer and served there for about two years. In 2012 fall, he enrolled in the Master of Science program in Chemical Engineering at North Carolina A&T State University. While pursuing his MS degree, Mr. Moniruddin worked as a research assistant of NSF CREST Bioenergy Center at North Carolina A&T State University. After completion of his MS degree, he will pursue his Ph.D. in Chemical Engineering at Texas Tech University, Lubbock, Texas.

Dedication

I would like to dedicate my thesis to my beloved parents, Jobyda Begum and Md. Helaluddin.

Acknowledgements

At first, I would like to express my sincere appreciation and gratitude to my advisor Dr. Shamsuddin Ilias for his excellence in scientific guidance, insight and continuous support. It has been an amazing experience, and I had tremendous personal and professional growth under Dr. Ilias's supervision. I am also thankful for the thesis committee members Dr. Vinayak N Kabadi and Dr. Jianzhong Lou for their valuable comments and suggestions.

I would like to give special thanks to Syed Zahadul Islam (former student of Dr. Ilias lab) for his continuous support, technical and experimental feedback. I am very much indebted to Syed Zahadul Islam for all the encouragement and more importantly for his friendship.

I am also thankful to Dr. Vishwanath Deshmane for his continuous technical support, and assistance to do the sample characterization. Analytical support from the Engineering Research Center (ERC), NCAT, is greatly appreciated with special thanks to Dr. Jag Sankar, Dr. Sergey Yarmolenko, and Dr. Zhigang Xu.

The financial support received from the National Science Foundation, NSF grant No. HRD-1242152 is gratefully acknowledged. I would like to thank all the faculty members and students of NSF Crest Bioenergy Center at North Carolina A&T State University, especially Dr. Debashish Kuila for his valuable comments and suggestions. I am indebted to North Carolina A&T State University for giving me the opportunity for graduate education and research. It has been a rewarding and learning experience.

I am grateful to my parents Zobyda Begum and Md. Helaluddin for their everlasting love and support. I would also like to thank my sister Aysha Akter for her continuous mental support and love. I would like to thank my friends, especially Md. Ariful Hoque, for his generous friendship and sharing for the last two years of my overseas life. Thank you.

Table of Contents

List of Figures

List of Tables

Abstract

Uses of fossil fuels in transportation and power generation release greenhouse gases. Hydrogen has the potential to be an alternative clean energy carrier. Hydrogen fueled proton exchange membrane fuel cell (PEMFC) can be used in transportation and stationary power generation to reduce greenhouse gas emissions. However, high purity hydrogen is required for PEMFC. In the current work, dense Pd-Ag composite membranes with an oxide layer on microporous stainless steel substrate (MPSS) were fabricated by surfactant induced electroless plating (SIEP) process for hydrogen separation. Prior to palladium/silver metal deposition, the MPSS disc was oxidized in stagnant air at 500 ºC for 18 h. A cationic surfactant, dodecyl trimethyl ammonium bromide (DTAB) was used in Pd- and Ag-bath for the sequential deposition of metals on MPSS substrates to remove the gas bubbles (N_2 and NH_3) produced during electroless plating. In this work, 4 CMC and 0.3 CMC (1 CMC = 15.6 mM) of DTAB were used in Pd- and Ag-bath respectively. Addition of a high amount of DTAB leads non-uniform Ag deposition and takes longer time to fabricate defect free Pd-Ag membrane. However, the average particle sizes were found to be 1.4 µm to 2.5 µm, which were relatively larger than the Pd-Ag film particle size using 4 CMC of DTAB in both Pd- and Ag-bath. Morphological features of the fabricated Pd-Ag membranes at pre- and post-annealing conditions were studied by using SEM, XRD, and EDS. The Pd-Ag membrane with an oxide layer showed higher permeability and selectivity in comparison to the membrane without oxide layer. However, at elevated temperature (550 ºC) the membrane showed a sharp decline in selectivity. The hydrogen flux and selectivity (H_2/N_2) of SIEP fabricated Pd-Ag membrane with an oxide layer were found to be 25.83 m^3/m^2-h and 500 respectively at 40 psi and 450 ºC.

CHAPTER 1

Introduction

Currently, the main energy system in the world is based on fossil fuels that are not renewable sources of energy. The global energy demand is increasing day by day, therefore escalating the concern about energy supply security [1]. Uses of fossil fuels as an energy source in transportation and power generation releases greenhouse gases. Their detrimental effects on the environment and consequent global climate change have been intensifying the concern to shift the energy sources from fossil fuels to alternative clean energy carrier.

It is now widely regarded that hydrogen as an alternative clean energy carrier has the capability of assisting in issues of environmental emission, sustainability, and energy security [1], [2]. According to DOE 2012 data, the United States produces about 9 million metric tons of hydrogen annually which is enough to power approximately 36~41 million fuel cell efficient vehicles [3]. Proton exchange membrane fuel cell (PEMFC) provides the technology to use this hydrogen energy in a highly efficient way in transportation and power generation, with only water and heat as byproducts. The use of hydrogen in fuel cell offers significant reduction of CO_2 emission and ending dependence on imported oil. High purity hydrogen is the fuel of choice for PEMFC.

Hydrogen is the third most abundant chemical in earth's crust and found invariably in chemical compounds such as with oxygen in water, petroleum, and natural gas [2]. Therefore, hydrogen must be produced from these resources to utilize it as an energy source. Hydrogen can be produced from several feedstocks such as biomass and fossil fuels like natural gas, coal, and petroleum. Various process technologies are available for hydrogen production including steam reforming, partial oxidation, auto thermal reforming, steam iron, plasma reforming,

thermochemical water splitting, and biological processes [4]. Among them steam reforming of methane or methanol are the most exercised industrial process [4]. From steam reforming reaction CO, CO_2, CH_4, and N_2 are produced as byproducts with H_2. As a result, it is necessary to separate hydrogen considering the end user's perspective. There are several existing processes for hydrogen separation such as pressure swing adsorption, cryogenic distillation, and membrane based separation.

Among the existing processes, membrane separation process is a very attractive alternative technology considering high purity hydrogen production at a lower cost [5], [6]. One of the major advantages of using membrane in hydrogen production process is that it can act as reactor-separator in simultaneous production and separation of hydrogen at process condition via process intensification [7]. There are three major categories of Hydrogen selective membrane based on the materials used: a) polymeric membranes, b) ceramic membranes, and c) metallic membranes. Polymeric membranes are highly selective but have limited mechanical strength and restricted to high temperature application, therefore are not suitable for the steam reforming reaction. Ceramic membranes have higher mechanical strength and thermal stability. Lastly, higher selectivity and thermal stability of metallic membranes makes it more attractive in the application of hydrogen separation [5].

In this context, Pd/Pd composite membranes on the porous substrate are best suited for hydrogen separation. Vycor glass, porous alumina, and porous metal are some common materials used as membrane substrate. Among them porous stainless steels offer several benefits including the sturdiness, weldability, closer thermal expansion coefficient to Pd, and can easily set in the industrial assemblies than fragile ceramic supports [8], [9]. Pd, Ni, and Pt have outstanding characteristics to dissociate and dissolve the hydrogen; therefore, they are best suited metals for

membrane application[10]. However, membranes made of Pd have higher capability to transport hydrogen through the metal because of their high hydrogen solubility over a wide range of temperature [11]. Despite high hydrogen permeability, palladium membranes have some limitations: a) α- to β-phase conversion in exposure to hydrogen at or below 298 ºC causes bulk and grain boundary defects, and b) hydrogen embrittlement during thermal cycling [11].

Pure Pd membrane limitations can be addressed by alloying Pd with other's metal such as Ag, Cu, Au, Y and Ru [11], [12], [13]. Among them, Pd-Ag membranes draw the researcher attention most because of alloying Pd with Ag lowering the α- to β-phase transition temperature, and at a certain composition (23 wt % Ag) Pd-Ag membrane shows the higher hydrogen permeance than pure Pd membrane [14].However, the fabrication of defect free Pd-Ag membrane and its reproducibility as well as long term stability are still challenges in this area.

There are several methods to synthesize Pd/Pd-alloy composite membranes such as chemical vapor deposition, magnetron sputtering, physical vapor deposition, electroplating and electroless plating. The current work's target was to fabricate defect free Pd-Ag membrane using electroless plating process. The problem associated in fabrication of Pd-Ag membranes by electroless plating methods are control of microstructure and pinhole formation which decrease the selectivity. As a result, membrane thickness is needed to be high enough to synthesize dense and defect free membrane. However, it is observed in the literature that hydrogen permeance decreases with membrane thickness. To control the microstructure of deposited thin Pd film, Dr. Ilias previous research group has patented a process called surfactant induced electroless plating (SIEP) [15]. Another research group of Dr. Ilias lab extended SIEP process to fabricate Pd-Ag membrane [16]. They used same concentration of surfactant (4 CMC of DTAB) in Ag bath based on the assumption that 4 CMC of DTAB in Ag bath will act similarly as it does in Pd bath.

However, the use of 4 CMC of DTAB in Ag bath decreases the plating rate and leads poor surface coverage. In this research, the purpose was to observe how different compositions of surfactant affect the microstructure and the performance of the Pd-Ag membrane. Another purpose was to investigate the behavior of Pd-Ag membranes introducing an oxide layer as a diffusion barrier fabricated by SIEP. In summary, the major tasks that had been done to fulfill the above mentioned objectives were:

1) To fabricate dense Pd-Ag membranes on MPSS by SIEP process with an oxide layer as a diffusion barrier. Pre- and post- heat treated membranes were characterized by SEM, XRD, and EDX to understand the morphology of the deposited film.

2) To fabricate dense Pd-Ag membranes on MPSS by SIEP process using different compositions of surfactant to understand the effect of surfactant on microstructure, and
3) To investigate H_2 permeability of Pd-Ag membranes to study the hydrogen transport at the temperature range of 250–550 ºC and at the trans-membrane pressure range of 20–100 psi.

This thesis is organized in five chapters, including introduction, Chapter 1. Literature review pertinent to this research is presented in Chapter 2. Then, materials and methods are described to fabricate Pd-Ag membrane in Chapter 3. First part of Chapter 4 discusses about the microstructure analysis of the Pd-Ag membranes along with full characterization where the later part of Chapter 4 discusses the performance of Pd-Ag membranes, in terms of H_2 transport behavior, and gas separation criterion. Finally, Chapter 5 gives the conclusion and some recommendations for future work.

CHAPTER 2

Literature Review

2.1 Introduction

Hydrogen can be used as an energy carrier alternative to fossil fuel which has the ability to address the issue of energy security, global climate change due to greenhouse gases, and local air pollution [17]. In recent years, hydrogen demand is growing continuously which motivated the research in development of hydrogen production and separation [18]. Regardless of the production process, hydrogen needs to be separated from other byproducts and therefore hydrogen separation is a key step in high purity hydrogen production system.

There are several industrial process exits for gas separation such as pressure swing adsorption, cryogenic distillation, polymer membrane diffusion, metal hydride separation, and membrane separation. The selection of process for the gas separation depends mostly on the product purity, and recovery percentage. Pressure swing adsorption is widely used in industrial scale to separate hydrogen from the mixture of gases. The advantages of this process are to bring down the impurities in the lower level and produce high purity of hydrogen (99.99 %) [5]. Cryogenic distillation is a very low temperature process, therefore, required a high amount of energy. However, very high purity hydrogen is not practical with this system. Other than pressure swing adsorption and cryogenic distillation, membrane separation process has drawn the researcher interest due to its low energy consumption, low operating cost, and minimizing unit operation [19]. Moreover, membrane has the capability to act as a reactor-separator unit for the simultaneous production and separation of hydrogen via process intensification. Palladium based membranes are the strong contender for this application. The comparisons among various gas separation technologies are given in Table 1.

Table 1

Comparison of H_2 Separation Technology [19]

Technique	Principle	Typical feed gas	Hydrogen output (%)		Scale of use	Comments
			Purity	Recovery		
Pressure swing adsorption	Selective adsorption of impurities from gas stream	Any hydrogen rich gas	99.999	70-85	Large	The recovery is relatively low as hydrogen is lost in the purging step
Cryogenic distillation	Partial condensation of gas mixture at low temperatures	Petrochemical and refinery off-gases	90-98	95	Large	Pre-purification step necessary to remove CO_2, H_2S, and water
Palladium membrane diffusion	Selective diffusion of hydrogen through a palladium alloy membrane	Any hydrogen containing gas stream	$\geq$ 99.9999	Up to 99	Small to medium	Sulfur-containing compounds and unsaturated hydrocarbon impair permeability
Metal Hydride Separation	Reversible reaction of hydrogen with metals to form hydrides	Ammonia purge gas	99	75-95	Small to medium	Hydrogen absorption poisoned by O_2, N_2, CO and S
Polymer Membrane Diffusion	Differential rate of diffusion of gases through a permeable membrane	Refinery off-gases and ammonia purge gas	92-98	> 85	Small to large	He, CO_2 and H_2O may also permeate the membrane

2.2 Pd Membrane for Hydrogen Separation

Membranes are defined as an inter-phase between two bulk phases, that act as a selective barrier and allows only the passages of a specific constituent from the feed bulk phase [4]. The bulk phase containing the components that permeate through membrane is called permeate side and the bulk phase containing the retentate components is called retentate side. Ability to dissociate and dissolve hydrogen is the key characteristics of a metal to act as a membrane for hydrogen separation. In the periodic table, metallic components belong to group 10 (Ni, Pt and Pd), and some elements in groups 3-5 have the ability to dissociate and dissolve the hydrogen. Figure 1 shows the hydrogen solubility of different metallic components [11]. Solubility is given in units of standard cm^3 of H_2 per 100 g of metal.

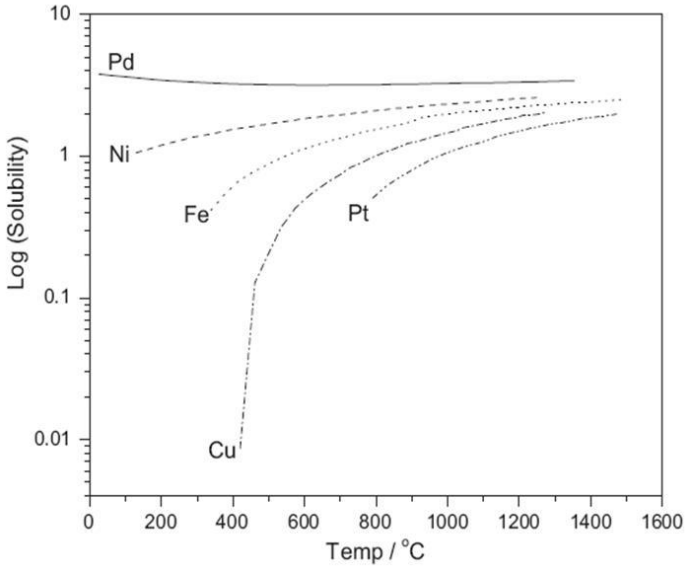

Figure 1. Comparison of hydrogen solubility in several metals at 1 atm.

Because of having higher hydrogen solubility of Pd over a wide range of temperature, only Pd membranes show the outstanding ability to diffuse hydrogen through it. As Pd membrane has higher hydrogen diffusion rate, therefore, Pd membranes have significantly drawn the attention of researchers for hydrogen separation and purification.

2.3 Hydrogen Permeation through Pd Membrane

Broadly, gas separation mechanism can be classified into four categories: a) Knudsen diffusion, b) molecular sieving, c) surface diffusion, and d) solution diffusion [20]. Knudsen diffusion occurs when the pore diameter of the effective barrier layer is smaller than the free mean path of the gas molecule being separated. Molecular sieving occurs based on the relative pore size of barrier layer and gas molecules. Surface diffusion becomes dominant when the gas molecule is adsorbed on the membrane surface significantly. Due to the concentration gradient, gas molecules diffuse through the bulk of the solid surface. In solution diffusion mechanism, gas molecules are separated based on the solubility and diffusivity of the gas molecules in the effective solid barrier. The mechanism of hydrogen permeation through the dense palladium membranes follows solution diffusion mechanism. The steps involved in hydrogen transport through the palladium membranes are: 1) diffusion of molecular hydrogen to the surface of the palladium membrane on high pressure side, 2) reversible dissociative adsorption on the palladium surface, 3) dissolution of atomic hydrogen into the bulk metal, 4) atomic hydrogen diffusion through the bulk metal, 5) association of hydrogen atom on the palladium surface, 6) desorption of molecular hydrogen from the surface on the low pressure side, and 7) diffusion of molecular hydrogen away from the surface [21]. The transport phenomena depicted in Figure 2. Each of the steps is characterized by an intrinsic forward and reverse rate. If one step becomes slower than the others, than the slower step control the overall hydrogen permeation [22]. The H_2 transport solution-diffusion mechanism can be described by the following equation [23]

$$N_H = \frac{Q_{H_0}}{t} \exp\left(-\frac{E}{RT}\right)\left(P_f^n - P_p^n\right) \quad (1)$$

where N_H is the molar flux of hydrogen (mol m^{-2} s^{-1}), Q_{H_0} is H_2 permeability through pure palladium film (mol m^{-1} s^{-1} Pa^{-n}), *t* is the membrane thickness (m or μm), E is the activation energy (J mol^{-1}), R is the universal gas constant (J mol^{-1} K^{-1}), *n* is the Sievert's law index, and P_f and P_p are the partial pressures of hydrogen on the high and low pressure sides (Pa), respectively. The value of index *n* depends on the limiting transport mechanism of hydrogen permeation through palladium or its alloy membrane.

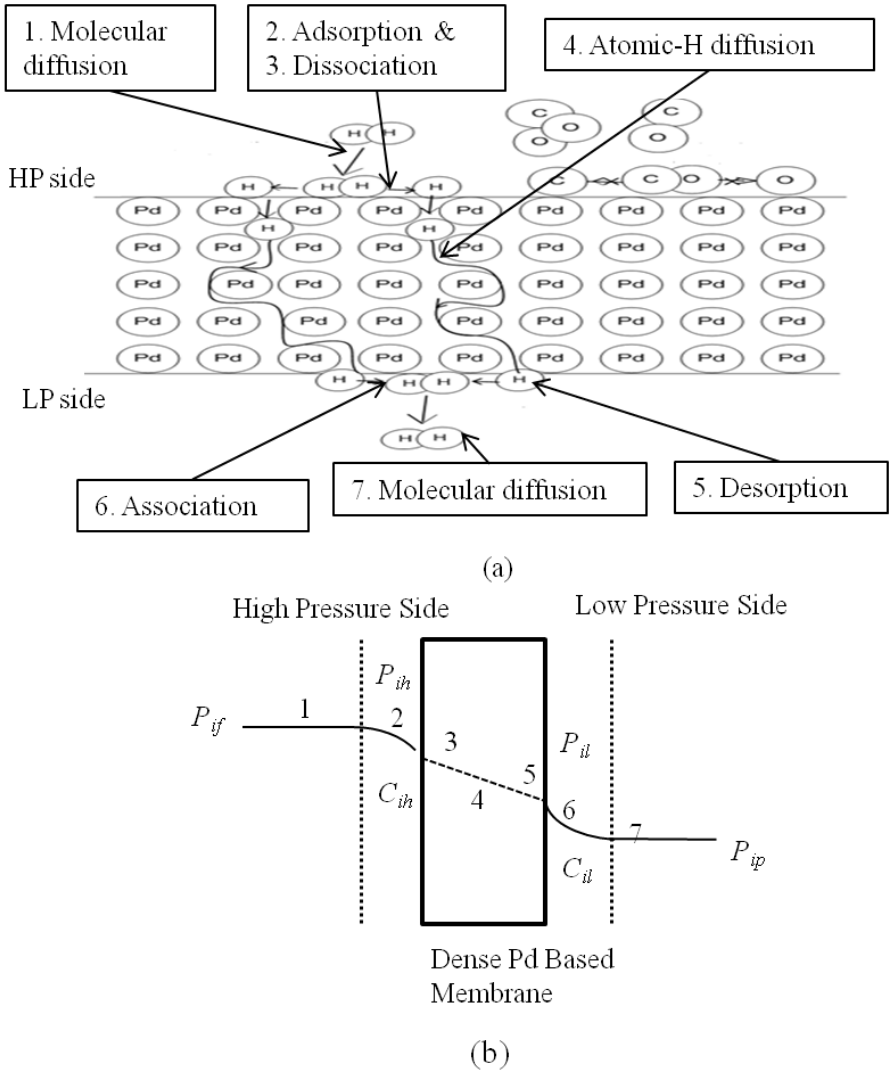

Figure 2. Transport mechanism of hydrogen through Pd membrane [16].

2.4 Metallurgical Properties of Pd and its Alloy Metals

Understanding the metallurgical properties of palladium is very important to implement palladium membranes as a hydrogen separation unit in the process of simultaneous hydrogen production and separation. In this context, many studies are conducted to understand the palladium-hydrogen or palladium alloy-hydrogen system. The palladium hydrogen phase diagram is given in Figure 3.

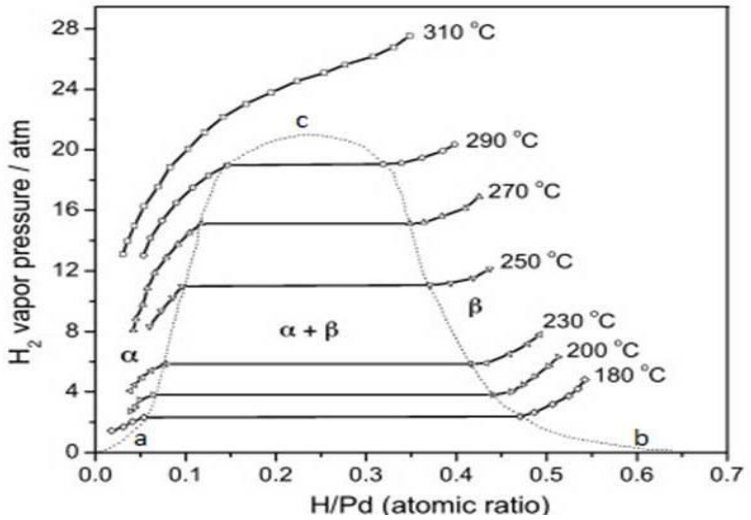

Figure 3. Phase diagram of palladium-hydrogen system [24].

As depicted in Figure 3, Pd hydride has two phases named α-phase, which dominates in low hydrogen concentration, and β-phase, which dominates in high hydrogen concentration. This two phase makes an envelope a-b-c. Phase transition is one of the important characteristics of Pd-H phase diagram which occurs in hydrogen concentration within palladium bellow the critical temperature and pressure of 298 ºC and 20 psi respectively [25]. In Figure 3, line a-c represents α_{max} that shows the maximum solubility of hydrogen in α-phase, and line b-c represents β_{min} that shows the minimum solubility of hydrogen in β-phase. In the abc region, both α- and β-phase coexist, and there is a continuous transformation from α- to β-phase with an increase of hydrogen concentration. Both of the phases have the same pure Pd face-centered cubic lattice and only

differ in their lattice constants. It is observed that at room temperature the crystal unit cell lattice parameter of hydrogen free Pd increases from 0.3890 nm to 0.3895 nm for the α-phase and up to 0.410 nm for the β-phase [19], [26]. Hydrogen permeability in the β-phase region is found higher than the α-phase and reached a maximum value around 200 ºC. However, it is undesirable to operate Pd membrane in this condition due to the phase transition which causes lattice strain and results in distortion, dislocation multiplication, and hardening of Pd membrane. Thus, consecutive hydrogen adsorption/desorption cycle below the critical point causes grain defects and complete loss of hydrogen selectivity. This phenomenon is called hydrogen embrittlement [27]. Hydrogen embrittlement can be minimized by operating the membrane above 300 ºC in hydrogen atmosphere and ensuring the cooling of membrane at dehydrogenated conditions [19]. However, this approach will narrow down its application.

In this context, Pd can be alloyed with other metallic elements such as Ag, Cu, Au, Ni, Pt and Y to alleviate embrittlement [11], [12], [13]. Using Pd alloy film as a membrane offers several benefits including minimizing hydrogen embrittlement by lowering critical temperature, higher permeability in comparison to pure Pd membrane, and cost reduction. Several studies show that hydrogen permeability depends on average bond distance of alloys in case of binary system. The larger atomic distance facilitates the hydrogen permeation process as it controlled by the diffusion of atomic hydrogen through the metal lattice [23].

Addition of Cu in Pd considerably minimizes the α- to β-phase transition, increases permeability and sulfur tolerance [28], [29]. Addition of 40 % (wt) Cu in Pd increases the permeability up to 1.5 times of pure Pd membrane at 350 ºC [30]. Alloying of Au with Pd also reduces the embrittlement phenomenon and increases sulfur resistance. Addition of 15 % (wt) Au in Pd gives higher permeability than pure Pd membrane [30]. Many works have been done on

Pd-Ag alloy due to its higher permeability and thermal stability compared to pure Pd membrane [19]. Hydrogen solubility increases with the Ag % (wt) and becomes higher at 23 % (wt) Ag, whereas, hydrogen diffusivity decreases with increasing of Ag % (wt). At 350 ºC and 23 % (wt) Ag in Pd shows 1.7 times higher hydrogen permeability than pure Pd [14]. Hydrogen permeability data for different palladium alloys have shown in Figure 4.

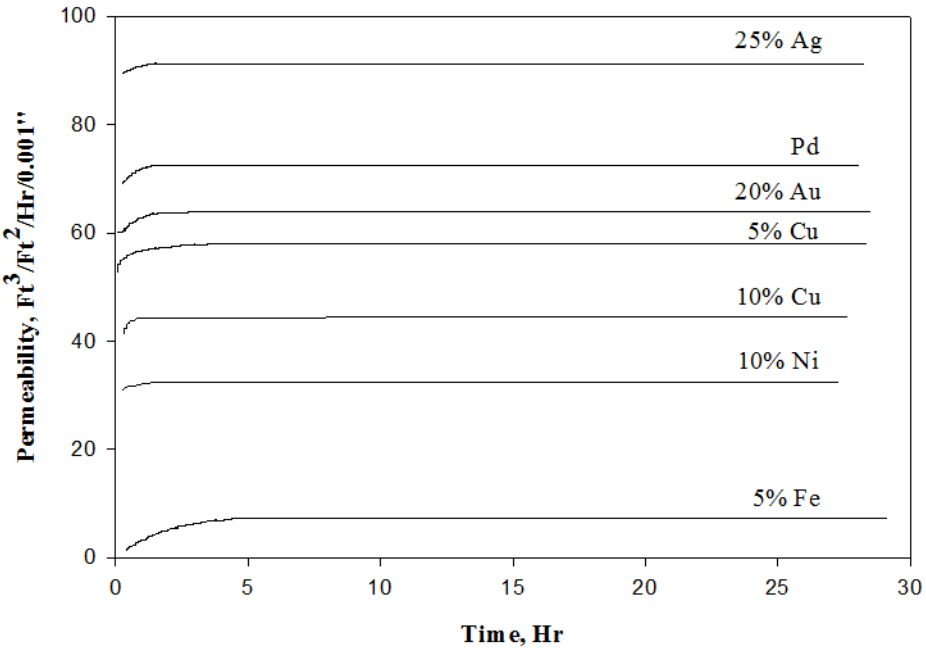

Figure 4. Rate of diffusion of hydrogen in palladium and number of palladium binary alloys (T = 540 ºC and P = 50 psi)[19].

2.5 Phase Diagram Analysis of Pd and Pd-Ag System

One of the major problems in Pd/Pd alloy composite membrane is the intermetallic diffusion of support metals (Fe, Cr, Ni) into the dense Pd active layer which causes low hydrogen permeation and non uniform Pd layer at higher temperature. Analysis of the phase diagram is necessary to understand the different metal-metal interaction or single metal phase behavior at various temperatures. For the fabrication of Pd-Ag membrane on MPSS, three

different systems: a) Pd-PSS binary system, b) Ag-PSS binary system, and c) Pd-Ag-PSS ternary system are important to investigate thoroughly. These phase diagrams help us to select the suitable temperature during the annealing process and give the information of intermetallic diffusion. The Pd-Fe phase diagram has given in Figure 5.

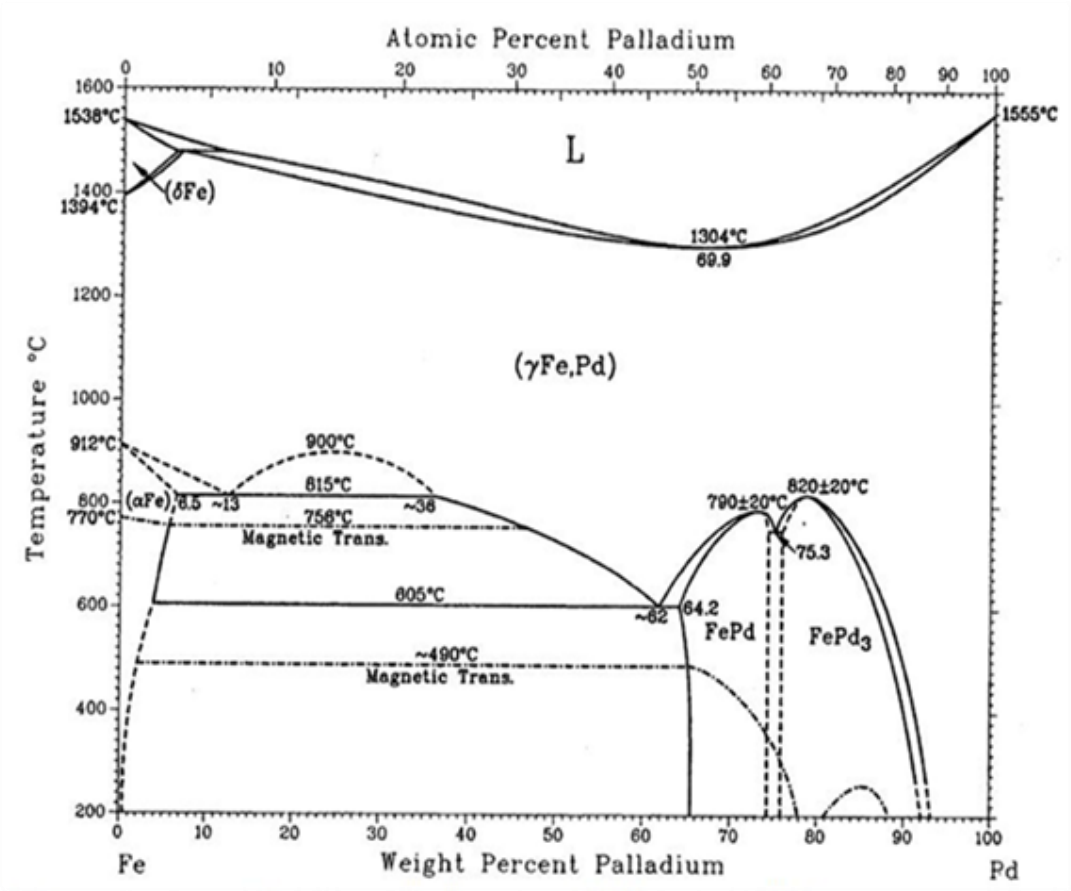

Figure 5. Phase diagram of palladium-porous stainless steel system [31].

Pd-Fe phase diagram has two important characteristics. First, the phase separation occurs in the Fe rich region less than 10 % (wt) Pd due to the size mismatch among αFe-, δFe-, and γFe-phases. Second, there are two ordered phases namely FePd and $FePd_3$ exist in the Pd rich region greater than 62 % (wt) of Pd bellow 800 ºC [32]. However, a continuous solid solution of Pd and γFe exists over the entire composition range of Pd at higher temperature (900 ºC). The Ag-Fe

phase diagram (Figure 6) has depicted that both in the solid and liquid phase the mutual solubility of Ag or Fe is very low, and no stable alloys of appreciable compositions form under the equilibrium conditions [33].

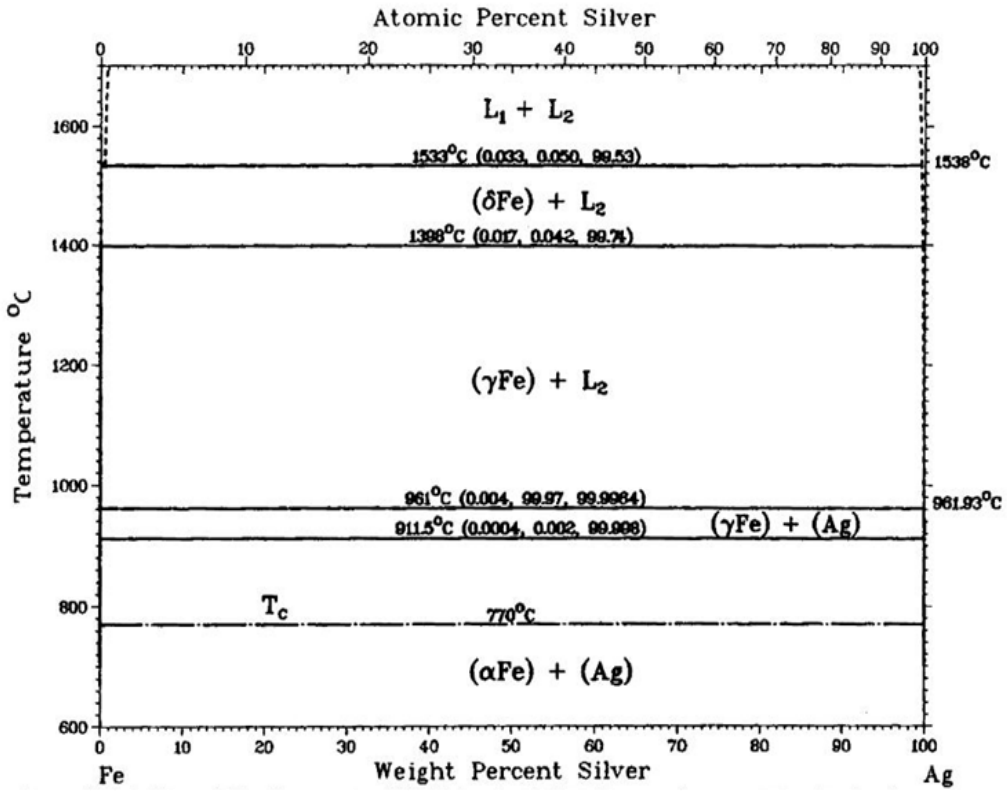

Figure 6. Phase diagram of silver-stainless steel system [34].

The maximum solubility of αFe in Ag is 0.0065 % (atomic) and the solubility of Ag in αFe is 0.0002 % (atomic) as reported in the literature [35]. In the Pd-Ag-PSS ternary system, annealing below the Tammann temperature ($T_{Tammann}$ = 640 ºC for Pd and $T_{Tammann}$ = 550-560 ºC for PSS 316L) forms Pd rich Pd-Ag alloy phase, whereas, annealing above the Tammann temperature produces simultaneously Pd rich Pd-Fe and Pd rich Pd-Ag phases. Ag rich Pd-Ag and Fe rich Pd-Fe phases are also observed if the annealing temperature goes beyond both the Tammann temperature. It is also observed that the Pd rich Pd-Fe layer between the support and the Pd-Ag barrier layer interface is not harmful to the permeability of the hydrogen [8].

2.6 Pd and Pd-Alloy Membranes Fabrication Techniques

Pd and Pd-alloy membrane can be synthesized by using various techniques such as chemical vapor deposition, physical vapor deposition, electroplating deposition, and electroless plating. Among them, electroless plating method can deposit palladium onto a metal substrate of any geometric shape and type (conductive or non conductive) more economically. A short description of each method is given below.

2.6.1 Chemical vapor deposition. Chemical vapor deposition (CVD) is a method where a volatile precursor of coating materials is thermally decomposed adjacent to the heated substrate to form a thin film [36]. Ye et al. [11] first reported this method for the formation of a Pd composite membranes using $PdCl_2$ as precursor on α-Al_2O_3 disk as substrate. In CVD method, it is necessary to have Pd precursor having high volatility and good thermal stability which are the key characteristics for short processing time and high yield [37]. Generally, precursors used for this method are $PdCl_2$, Pd(acetylactonate)$_2$, Pd(C_3H_5)$_2$, Pd(C_3H_5)(C_5H_5) and Pd(C_5H_5)$_2$ [38]. One of the major advantages of this fabrication method is better film quality and capability of fabricating very thin (< 2 μm) Pd or Pd alloy films [11]. The limitations of CVD method are requirement of high purity constituents and strict process conditions, high cost of the precursors, and contamination of the film by the constituents of organometallic complex such as carbon.

2.6.2 Physical vapor deposition. In Physical vapor deposition (PVD) processes, the targeted metal is vaporized from a solid precursor at an atomic level and vaporized atoms are transported through a vacuum or low pressure gaseous environment to the substrate, where it condenses [39]. PVD techniques are very useful to deposit thin film of single metal or alloy. PVD is similar to CVD except that chemical decomposition reactions are not occurred in the surface reactions because in PVD the precursors are pure metals in the elemental state and in

CVD the precursors are chemical compounds in a vaporized state [39]. The main categories of PVD process are magnetron sputtering deposition, vacuum deposition, arc deposition, and ion plating. A PVD technique provides better control of the film composition, phase and thickness. However, the equipment used in PVD process is usually expensive due to the requirement of high vacuum and power density to evaporate the target material. In addition, the geometry of the substrate is also limited to a flat shape which restricts its practical applications.

2.6.3 Electroplating deposition. Electroplating deposition (EPD) is an electrochemical process in which metal ions from the electrolyte deposited upon a substrate by the act of electric current. In EPD process, substrate act as a cathode and the positive metallic ions are reduced to metal and deposited on the substrate. This method requires very simple equipment and can easily control the film thickness by controlling electroplating time and current density [40]. However, it is not possible to deposit metal on nonconductive substrate by this method. It is suitable for the conducting support materials such as stainless steel.

2.6.4 Electroless plating. Electroless plating (ELP) is a method in which metal deposited on a substrate by the reduction of metal complex ions in solution with the help of a chemical reducing agent without applying any external electric current. ELP can produce films of metals, alloys, compounds, and composite on both conductive and nonconductive substrate. It provides several advantages such as ability to deposit metals on surfaces of complex geometry, good adhesion to the substrate, and require simple equipment and low investment [41]. Thus, it is widely used in the area of circuit boards, radio frequency interference shielding for computers, corrosion and wear resistant metal surfaces, lightweight plated plastics, and membrane fabrication processes. Kikuchi et al. and Uemiya et al. first applied this technique to fabricate Pd and Pd alloy composite membranes [42]. Some major drawbacks of ELP are that the process

involved several steps and time-consuming in nature, and it uses toxic chemicals and generate hazardous liquid waste.

2.7 Substrate Materials and its Modification for ELP

Palladium itself without any support such as palladium foil can act as a membrane for hydrogen separation. Due to low mechanical strength palladium foil thickness should be high enough, but thicker palladium layer decreases hydrogen permeability. Different types of substrate such as vycor glass, ceramics, and stainless steel are used to lower the membrane cost and as well as to increase the hydrogen permeability and selectivity [11]. Porous vycor glass supports are capable of withstanding at high temperature along with high porosity but are mechanically fragile [11]. Porous ceramic supports have several benefits as a substrate for Pd composite membrane. The advantages of ceramic substrates are: a) they can form into a variety of shapes with controllable pore sizes, b) they have higher thermal and mechanical stability, and c) they facilitate high hydrogen permeability [43]. Currently, metals are widely used as a substrate for the fabrication of Pd membranes. Sturdiness, the ability to weld, closer thermal expansion coefficient to that of palladium, and ease of fabrication due to conductive property makes stainless steel more attractive than others support materials [43], [44].

It has been reported that the substrate top layer features significantly affected the quality of the Ag/Pd deposition [45]. The intermetallic diffusion at the interface between the palladium film and the substrate at high temperature may deteriorate the performance of the palladium alloy membrane [46]. Using a diffusion barrier could prevent the intermetallic diffusion between the two neighboring layers. Ma et al. [47] introduced an oxide-layer as intermetallic diffusion barrier between the palladium alloy layer and the stainless steel substrate. Nam and Lee [8] introduced colloidal silica sol layer by sol gel techniques between the palladium alloy layer and the stainless

steel substrate as an intermetallic diffusion barrier. Wang et al. [48] modified the porous stainless steel support with zirconium oxide particles before Pd deposition. Ayturk et al. [49] developed a method named bi-metal multi-layer (BMML) deposition technique in which a porous Pd-Ag intermetallic diffusion barrier layer was introduced, prior to the hydrogen selective layer. Yepes et al. [46] used wash coating to make a thin film of γ-Al_2O_3 on the PSS surface.

2.8 Synthesis of Pd and Pd-Ag Membranes by Electroless Plating Process

Electroless plating is an autocatalytic deposition process and involves the presence of a chemical reducing agent in solution to reduce metallic ions to the metal state [50]. Electrochemically, an electroless deposition reaction is the combination of two independent electrode reactions named as cathodic partial reaction (i.e. metal ion reduction) and the anodic partial reaction (i.e. oxidation of reducing agent). The reducing agent supplied the electrons that required for the reduction of the metal ions. Common Pd metals sources for electroless plating are $PdCl_2$, $Pd(NH_3)_4Cl_2$, $Pd(NH_3)(NO_3)_2$, and $Pd(NH_3)_4Br_2$). $AgNO_3$ salt is the common source of Ag metal for the electroless plating process. In both Pd- and Ag-bath, ethylene-di-amine tetra-acetic acid (EDTA), ethylene-di-amine (EDA), and ammonium hydroxide (NH_4OH) are used as complexing agent and solution stabilizer. Hydrazine (NH_2NH_2), sodium phosphinate monohydrate ($NaH_2PO_2.H_2O$), and tri-methyl-amine-borane are some common reducing agents used in the electroless plating process [51].

The fabrication of Pd-Ag membrane involves several steps including pretreatment of substrate, activation of substrate and Pd or Ag electroless deposition. Activation of substrate helps to shorten the induction period for the autocatalytic decomposition reaction of the metastable complexes of Pd salts on the substrate and to initiate the electroless plating process.

In a conventional electroless plating process, the substrate is activated by acidic $SnCl_2$ and $PdCl_2$ solution. This activation and sensitization step can be described by the following reaction:

$$Pd^{2+} + Sn^{2+} \rightarrow Pd^{\circ} + Sn^{4+} \quad (2)$$

The reaction steps for Palladium and Silver deposition in electroless plating bath are shown below:

In Pd-bath,

$$2Pd(NH_3)_4^{2+} + 4e^- \rightarrow 2Pd^0 + 8NH_3, \qquad E^0 = 0.0\ V$$
$$N_2H_4 + 4OH^- \rightarrow N_2 + 4H_2O + 4e^-, \qquad E^0 = 1.12\ V$$

$$2Pd(NH_3)_4Cl_2 + N_2H_4 + 4NH_4OH \rightarrow 2Pd^0 + N_2 + 8NH_3 + 4NH_4Cl + 4H_2O \quad (3)$$

In Ag-bath,

$$4Ag(NH_3)_2^+ + 4e^- \rightarrow 4Ag^0 + 8NH_3, \qquad E^0 = 0.61\ V$$
$$N_2H_4 + 4OH^- \rightarrow N_2 + 4H_2O + 4e^-, \qquad E^0 = 1.12\ V$$

$$4Ag(NH_3)_2NO_3 + N_2H_4 + 4NH_4OH \rightarrow 4Ag^0 + N_2 + 8NH_3 + 4NH_4NO_3 + 4H_2O \quad (4)$$

Currently, hydrazine based electroless plating bath is very attractive. Rhoda first developed hydrazine based bath using $Pd(NH3)_4Cl_2$ as Pd metal source [52]. The observations reported by Rhoda [52] were: a) plating rate increased within the temperature range of 40-80 ºC and precipitation occurred in the absence of stabilizer EDTA salt above 70 ºC bath temperature, and b) plating rate decreased with time due to the catalytic decomposition of hydrazine by palladium. Based on his findings, hydrazine based electroless plating was studied by many research groups over the years and introduced modification to apply this process successfully in the fabrication of dense hydrogen selective Pd-composite membrane [51].

2.9 Surfactant Induced Electroless Plating (SIEP)

In conventional electroless plating (CEP), oxidation-reduction reaction between the Pd precursor and reducing agent (hydrazine) results in metallic deposition of Pd on a solid surface. During the electroless plating process, NH_3 and N_2 gas bubbles are produced from the oxidation-reduction reaction between Pd complex and hydrazine. These gas bubbles hinder uniform Pd-film deposition while adhering to the substrate surface and in the pores, which eventually create micro-porosity in the deposited film [15]. To improve the deposition characteristics and surface morphology of Pd and Pd-alloy layers, many researchers have introduced different techniques to the synthesis routes over the years and continuously modified the CEP technique. The modifications that reported in the literature are: (a) using osmosis in combination with electroless plating that produces smaller grain size and denser Pd film, (b) using combined method of ELP and CVD to repair the surface defects of Pd fabricated by ELP, and (c) stirring the plating bath solution or rotating the substrates at a certain speed to remove the mass transfer barrier during elertoless plating.

Introducing surface active compounds with suitable structures into the plating bath solution is another promising remedy to lessen the surface pinholes problem. Chen et al. [53] investigated the effects of surfactants in an electroless nickel plating-bath where hydrogen gas is evolved during the plating process. The observations reported by Chen [53] were (a) addition of a small amount of surfactant increases the deposition rate by 25 % compared to the surfactant free plating-bath, (b) surfactant can minimize the formation of micro pitting on the deposited film, and (c) excessive use of surfactant results in inferior surface quality and slow deposition rate. To address the similar issue, Ilias et al. investigated the palladium deposition on micro-porous stainless steel (MPSS) substrate in the presence of anionic, cationic, and nonionic

surfactants in ELP process, which they called surfactant induced electroless plating process (SIEP) [15], [54]. Among various types of surfactant, it was found that cationic surfactant effectively activates the process of grain nucleation and agglomeration in the deposition process. A cationic water soluble surfactant named dodecyl trimethyl ammonium bromide (DTAB) is found effective in this application. The role of surfactant in this process is to remove the adhered NH_3 and N_2 gas bubbles (plating bath reaction products) from the substrate surface and the pores to provide control of Pd-deposition rate and Pd-grain size distribution [54].

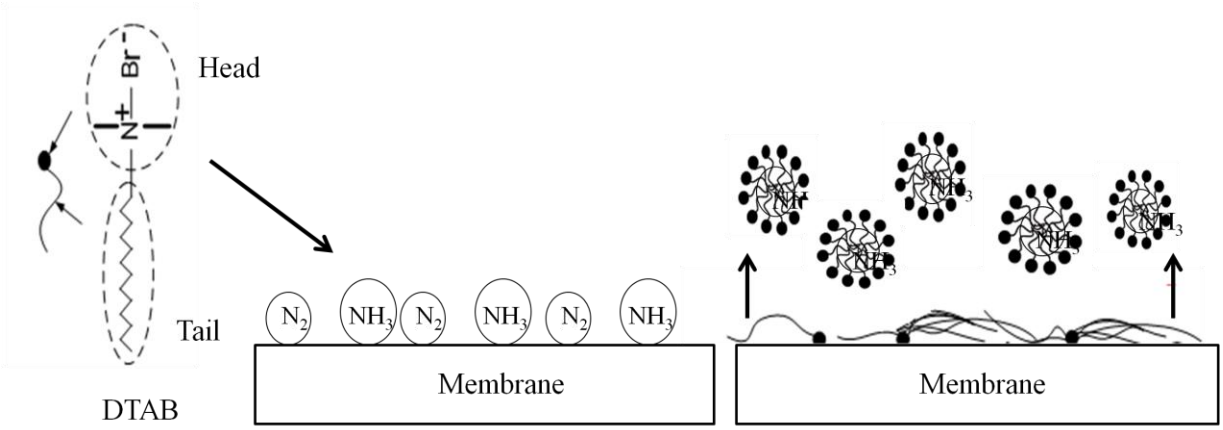

Figure 7. Hypothesized mechanism of gas bubbles removal by surfactant (DTAB) in SIEP.

In SIEP, the surfactant takes part in reduction reaction and reduces the plating time. However, how surfactant takes part in the reaction has not confirmed yet. It is hypothesized that the surfactant removes the gas bubbles by forming micelle. Micelles are formed above a certain surfactant concentration level which is called critical micelle concentration (CMC). The gas bubbles produced from the reaction bath (NH_3 and N_2) adsorbed on the substrate surface. The micelles reduced the surface tension between the bubbles and substrate; as a result, the gas bubble comes up from the substrate surface. As the surfactant removes the gas bubbles from the targeted surface, which ultimately leads uniform metal deposition during electroless plating.

In SIEP technique, the observations reported by Ilias et al. [55] were following: a) addition of surfactant decreases the Pd plating time compared to the surfactant free bath, b) using SIEP dense Pd membrane can be fabricated with lower thickness than conventional EP, and c) deposited Pd grains size were reduced from 8 μm (EP) to about 2 μm (SIEP). Table 2 and Figure 8 have shown the effect of different CMC of surfactant on the characteristics of Pd membrane fabricated by SIEP.

Table 2

Measured Pd-film Thickness by Weight-gain Method and SEM Cross-section Analysis of SIEP MPSS-Pd Composite Membranes [55]

Membrane Sample	DTAB Concentration (CMC)	Deposition Time (h)	Pd-film thickness (μm) measured by	
			Weight-gain	SEM analysis
Pd-MPSS (A)	0.5	22	23	22.5
Pd-MPSS (B)	2	16	17.8	18.3
Pd-MPSS (C)	3	13	14	13.5
Pd-MPSS (D)	4	10	8.5	8.5
Pd-MPSS (E)	0	28	28.5	27.5

Table 2 shows that the film thickness and plating time of the fabricated Pd membrane by conventional electroless plating becomes higher than SIEP. For Pure Pd membrane, 4 CMC of DTAB in reaction becomes more effective to reduce the plating time as well as film thickness.

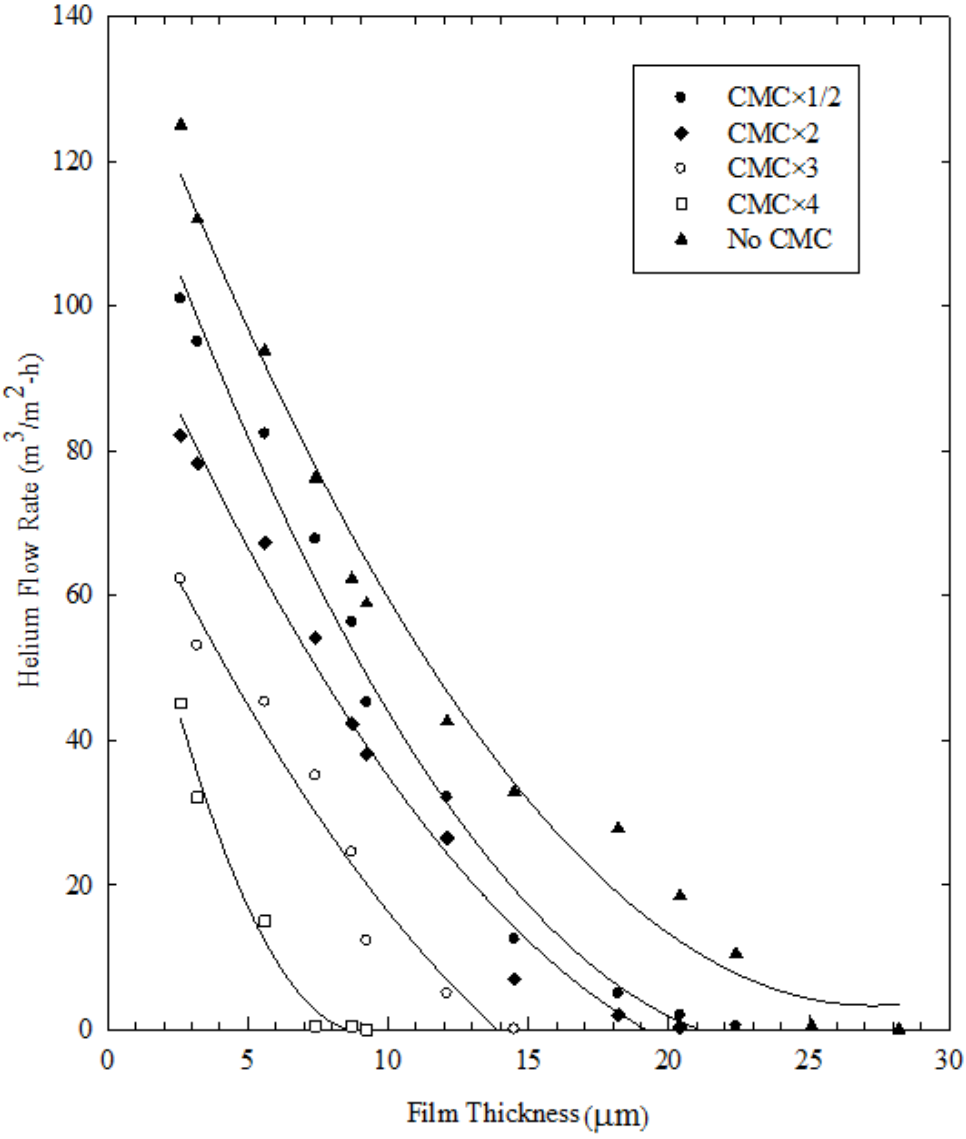

Figure 8. Helium flow rate as a function of Pd film thickness of different membranes fabricated at varied CMCs of DTAB surfactant [55].

Moreover, thermal stability test for SIEP produced Pd membranes were carried out and found thermally stable for a period of 1200 h under thermal cycling of 300 – 450 – 300 °C at 15 psi pressure [56]. Pd-Cu membrane was also found stable and retained hydrogen permeation characteristics for over three months of operation under the same condition [57].

2.10 Conclusion

SIEP is a modified technique of CEP. It offers higher hydrogen permeability with low thickness compared to the CEP membrane[15], [54]. Although many works have been done on Pd-Ag composite membrane by electroless plating method, in this research our interest is to study the Pd-Ag membrane properties fabricated by SIEP. It is believed that the surfactant will facilitate the uniform Pd/Ag deposition on MPSS substrate and reduce the membrane thickness with higher perm-selectivity. For fabricating Pd-Ag membrane, it is important to optimize the surfactant (DTAB) concentration in both Pd- and Ag-bath. In the previous work, the effective surfactant amount had already been established for Pd-bath. Therefore, to control the microstructure of the Ag it is essential to find out the optimum amount of DTAB in Ag-bath. The intermetallic diffusion between the deposited film and the MPSS substrate reduces the permeability. Substrate modified with oxide layer has the ability to prevent intermetallic diffusion. Therefore, an oxide layer can introduce at the interface between the substrate and deposited film for the comparative H_2 permeation study of Pd-Ag membrane with and without oxide layer.

CHAPTER 3

Materials and Methods

3.1 Membrane Synthesis

3.1.1 Substrate. Micro-porous stainless steel (MPSS, 316L) discs of grade were used as the substrate for membrane fabrication. Substrates were supplied by Mott Metallurgical Corporation, Farmington, CT. The dimension of the MPSS discs was 1 inch in diameter and 0.062 inch in thickness with average pore size of 0.2 µm as per manufacturer's product information. Figure 9 shows the photograph of the substrates.

Figure 9. Membrane support (MPSS 316 L disc).

3.1.2 Substrate pretreatment. In this work, combination of Islam [54] and Rahman [16] fabrication procedure were followed to synthesize Pd-Ag membrane. The fabrication procedure starts with the substrate cleaning. To remove any sticky particle or external dust the substrates were gently rubbed by a metal brush and followed by tape water washing. Then substrates were cleaned by a freshly prepared basic cleaning solution to remove oil, grease, corrosion products, and other's contaminants that adhered to the top surface of the substrate [58] Chemicals used for the cleaning solution are given in the Table 3. For cleaning, substrates dipped in the fresh cleaning solution (20 ml solution in 50 ml beaker) were kept in the ultrasonic bath for 30 min at 60 ºC temperatures and followed by washed with DI water. This cycle was repeated three times.

Due to the basic nature of the cleaning solution, substrates needed to wash thoroughly to make its surface neutral (pH 7). For surface neutralization, substrates dipped in the DI water were kept in the ultrasonic bath twice for 20 min each and followed by dipped in the isopropanol (fisher scientific) solution for 15 min. Finally, cleaned substrates were dried at 120 ºC overnight in an oven. For the oxide layer, substrates were oxidized at 500 ºC in stagnant air for the period of 18 h in an oven at a heating and cooling rate of 4 ºC per min.

Table 3

Chemical Composition of Cleaning Solution

Name of Chemicals	Supplier	Composition
$Na_3PO_4.12H_2O$ (ACS Reagent grade, 99.4 %)	Alfa Aesar	45 g/L
Na_2CO_3 (ACS Grade, ≥ 99.5 %)	Alfa Aesar	65 g/L
NaOH (ACS Grade, 97 %)	Alfa Aesar	45 g/L
Industrial Detergent (Liqui-Nox^R)	Alconox	5 ml/L

3.1.3 Sensitization and activation. Before Pd/Ag plating, substrates were activated by seeding with Pd nuclei to initiate the electroless plating process. Sensitization and activation solution were prepared by using reagent grade tin (II) chloride dihydrate (Sigma-Aldrich, 98 %) and palladium (II) chloride (Alfa Aesar, 99.9 %) in hydrochloric acid (ACS Reagent grade, 37 %). The chemical composition of the sensitization and activation solutions is given in Table 4. Before the activation steps, the bottom part and the periphery of substrates were sealed by paraffin film and scotch tape. The activation procedure consisted of first dipping the substrate in the sensitizing solution (20 ml solution in 50 ml beaker) for 5 min and then in activation solution (20 ml solution in 50 ml beaker) for another 5 min with an intermediate washing of DI water.

Intermediate washing helps to prevent drag out of sensitizing solution to activation solution, as well as by-products of Sn^{+} hydrolysis such as $Sn(OH)_{1.5}Cl_{0.5}$ and other hydroxyl chlorides [59]. After that, the cycle ends with dipping of the activated substrate in 0.1N HCl solution to prevent hydrolysis of Pd^{+} [59]. The complete cycle was repeated at least for 4 times until an uniform dark brown color appeared on the substrate surface [16]. Finally, activated substrates were dried in an oven for 1 h at 60 ºC.

Table 4

Chemical Composition of Sensitization and Activation Solutions

Name of Chemicals	Supplier	Sensitization Solution	Activation Solution
$SnCl_2.2H_2O$ (ACS Reagent grade, 98 %)	Sigma-Aldrich	1 g/L	-
$PdCl_2$ (ACS Reagent grade, 99.9 %)	Alfa Aesar	-	0.1 g/L
HCl (ACS Reagent grade, 37 %)	Sigma-Aldrich	1 ml/L	1 ml/L
Temperature		20 ºC	20 ºC
Time		4-6 min	4-6 min
pH		2-3	2-3

3.1.4 Pd and Ag electroless plating. After the activation of substrates with Pd nuclei, Pd and Ag were deposited sequentially by surfactant induced electroless plating method. The chemical composition of electroless plating Pd and Ag bath used in the lab are shown in Table 5. The preparation procedure for Pd /Ag bath solution (1 liter) consisted of adding Pd/Ag salt into 300 ml DI water and shake vigorously until complete dissolution. After the dissolution of Pd/Ag salt, Na_2EDTA (40gm) was added and dissolved completely then followed by adding 198 ml of NH_4OH (28 wt %) into the solution. Finally, DATB was added by shaking it gently until complete dissolution. The solution was then made 1 liter by adding DI water. In this research, Pd/Ag bath solution was prepared at least 5 h before the Pd/Ag electroless plating. Pd/Ag

deposition was carried out in an electroless plating bath at a temperature of 60 ºC. Firstly, the plating solution (20 ml solution in 50 ml beaker) was heated for 10 min in water the bath and then reducing agent N_2H_4 was added. After 1 min, substrates were dipped in the plating solution and kept there for 1 h. Each one h later solution was replaced by a fresh one to maintain the plating rate. In between the changing solutions, substrates were rinsed with hot DI water. No further deposition was performed after 3-4 cycles. When the deposition was complete, substrate were dipped into the hot DI water for 30 min at 80 ºC to make the substrate surface neutral (pH 7). Finally, substrates were dried in an oven at 120 ºC overnight. The whole procedure for activation to Pd/Ag deposition need to repeat several times until the He flux becomes zero. The plating process started with Pd layer and end with final Pd layer. In between, Ag and Pd layer were deposited sequentially and tried to maintain the weight ratio of Pd:Ag = 77:23.

Table 5

Chemical Composition of Pd-bath and Ag-bath Solutions

Name of Chemical	Supplier	Pd-bath	Ag-bath
$Pd(NH_3)_4Cl_2.H_2O$ (10 wt %)	Sigma-Aldrich	4 gm/L	-
$AgNO_3$ (ACS grade, ≥ 99.9 % metal basis)	Alfa Aesar	-	0.519 gm/L
Na_2EDTA (≥ 99 %)	Acros Organics	40.1 gm/L	40.1 gm/L
NH_4OH (ACS grade, 28 %)	Fisher Scientific	198 ml/L	198 ml/L
NH_2-NH_2 (1.0 M)	Sigma-Aldrich	5.6 mM	5.6 mM
DTAB (90 %)	Sigma-Aldrich	4 CMC	0.3-4 CMC
Time		60 min	75 min
Temperature		60 ºC	60 ºC
pH		11-12	11-12

3.2 Membrane Post Treatment

For the membrane annealing, the fabricated Pd-Ag membranes were heat treated in a gas tight diffusion cell. The set up was similar to the one reported by Islam et al. [54]. The heat treatment set up is shown in the Figure 10. During the heat treatment process, first, membranes were heated to a temperature of 500 ºC from the room temperature in the presence of nitrogen gas. At 500 ºC nitrogen gas was switched to hydrogen and kept the membrane for 18 h. After 18 h again hydrogen gas was switched to nitrogen and brought down the temperature to ambient condition. During the heat treatment period, the feed side pressure was always kept at15 Psi and the permeate side was equal to the atmospheric pressure. The ramping rate of temperature during heating and cooling was maintained 2 ºC per min.

3.3 Membrane Characterization

For microstructure analysis of the fabricated membranes, scanning electron microscopy (SEM) equipped with energy dispersive spectroscopy (EDS) was used. Grain sizes of the fabricated membrane were determined using point-to-point measurements from representative SEM images. Elemental quantification and EDX metal mapping was carried out on Zeiss EVO LS10 SEM equipped with OXFORD INCA X-act detector. The statistical distributions were estimated in a fixed cross sectional area of the membrane from the SEM image. The phase analysis of the membranes were carried out using Bruker D2 Phaser Diffractometer equipped with a 1D Lynxeye detector, utilizing Cu Kα (λ = 1.5405 Å) radiation, operated at 30 kV and 10 mA using a step width of 0.014° and a 2-theta range of 20° - 90°. H_2 permeability and selectivity studies were carried out at temperature range from 250-550 ºC and at 20-100 psi transmembrane pressures. Prior to the permeability test, the membrane was washed with hot DI water and iso-propanol solution respectively, and followed by 2 h drying under nitrogen environment. During

the permeability test, the temperature ramping was 5 ºC/min. The membrane was placed in diffusion cell using two graphite gaskets, one in top and the others in the bottom. The dimensions for both gaskets were OD = 25.6 mm and ID = 20 mm

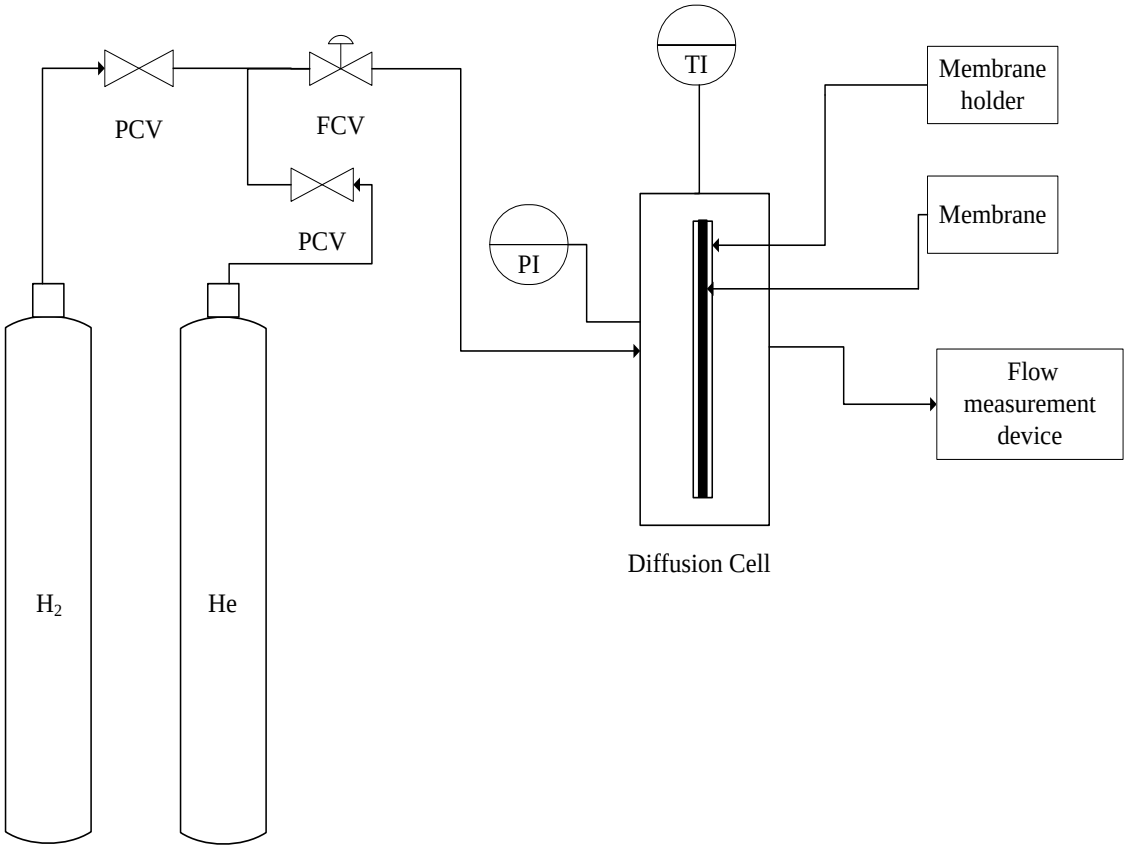

Figure 10. Experimental set-up for gas permeability test through membrane (FCV - flow control valve, TI - K - type thermocouple, PCV - pressure control valve)

.

CHAPTER 4

Results and Discussions

4.1 Introduction

In this research, Pd-Ag composite membranes with an oxide layer on MPSS were fabricated by SIEP process. Successful fabrication of thin, dense and defect free Pd-Ag composite membrane largely depends on the deposited Pd or Ag layer microstructure. The substrate surface roughness, fabrication technique, bath parameters, and operating conditions may have significant influence on the microstructure of Pd-Ag composite membrane. In this work, Pd-Ag composite membranes were fabricated by SIEP process using different concentration of surfactant (DTAB) in Ag bath while keeping the other parameters such as bath composition, bath parameters, operating conditions used in our previous work. An oxide layer also introduced to study the intermetallic diffusion characteristics and its effect on the hydrogen permeability. Two types of Pd-Ag membrane based on two different surfactant concentrations were studied in this work. In the first type, Pd-Ag membrane without oxide layer was fabricated by using 4 CMC of DTAB in both Pd- and Ag-bath. In the second type, Pd-Ag with oxide layer was fabricated by using 4 CMC and 0.3 CMC of DTAB in Pd- and Ag-bath respectively. In this work, second type of Pd-Ag membrane was fabricated by SIEP. All the data for first type membranes were taken as a reference from the previous work [16].

In the following section, membrane characterization and hydrogen permeability studies are presented to analyze the microstructure and performance of the Pd-Ag composite membranes. Instrumental analyses such as scanning electron microscopy (SEM), energy dispersive spectroscopy (EDS), and X-ray diffraction (XRD) were carried out to characterize the membrane for microstructure analysis, grain size distribution, grain agglomeration, and metal

composition. Hydrogen permeability tests were carried out at temperature of 250-550 ºC and transmembrane pressure of 20-100 psi.

4.2 Microstructure Analysis

4.2.1 Study of Pd-Ag membranes microstructure. The PSS disc was oxidized in stagnant air at 500 ºC for 18 h prior to palladium/silver metal deposition on the substrate surface. The oxide layer at the interface between palladium/silver metal and the substrate could function as the intermetallic diffusion barrier [47], [58]. The weight gain of the substrate was found 0.36 % of the original weight. Change of helium flux was measured 17.4 % after the oxidation that indicates a decrease in the porous size of MPSS substrate. Top surface SEM images of bare substrate and substrate with oxide layer (Figure 11) shows that that the oxidation does not constrict the internal pore system. The weight of the oxide layer depends on the oxidation temperature. The weight gain of the oxide layer increases with the oxidation temperature. However, the oxidation had little effect on the pore size of the MPSS even at 800 ºC oxidation temperature [60].

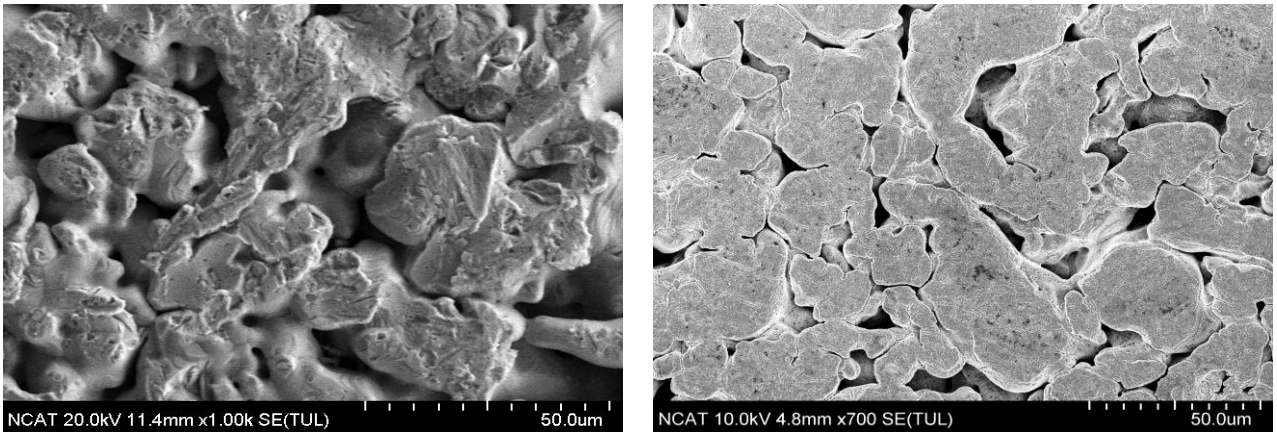

(a) (b)

Figure 11. SEM images of clean substrate (a) MPSS top surface [56] (b) Modified MPSS with oxide layer.

The surface topology of fabricated Pd-Ag film on MPSS was analyzed by SEM images. Figure 12 shows the top view of Pd-Ag membrane. For the fabrication of this Pd-Ag membrane, we followed the sequential SIEP process that ended with Pd deposition. The Pd-Ag film shows finer grain size as well as the agglomeration of the grains. Figure 13 also shows the top view of Pd-Ag membrane in which the sequential SIEP process ended up with Ag deposition. The apparent uniformity of the agglomeration is not that high as it was observed for pure Pd membrane in previous work [55].

To explain the non-uniformity of agglomeration in case of Pd-Ag membrane, we need to look at the fabrication process. The sequential steps of the deposited film were Pd-Ag-Pd-Ag-Pd. Deposition was made in such a way that the Pd to Ag weight ratio in each step was 77:23. Ag particle deposition has special trend. To examine the Ag particles deposition trend, one Pd-Ag membrane was prepared which consist of three Pd layers (60 min plating time each) and followed by three Ag layer (75 min plating time each). Figure 14 shows the SEM image of the top layer of Pd-Ag at different magnification. The Pd and Ag deposition morphology are completely different. From the Figure 14, we can confer that the Pd deposition covers the whole surface including the cavity areas of the substrate that is in agreement with the previous work [54]. In the case of Ag, little or no silver deposition was likely to have occurred in the cavity areas, which mean existence of dendritic growth of Ag. Therefore, they make elevated region surroundings the cavity that may be responsible for the non-uniform agglomeration of Pd-Ag membrane. Similar observations were also reported by Rahman [16] and Ayturk et al. [49]. So, the CMC of DTAB needs to be increased to prevent the dendritic Ag growth. It was observed that 4 CMC of DTAB in Ag-bath leads poor surface coverage and decreases the plating rate, and without DTAB the Ag-bath solution becomes unstable during electroless plating.

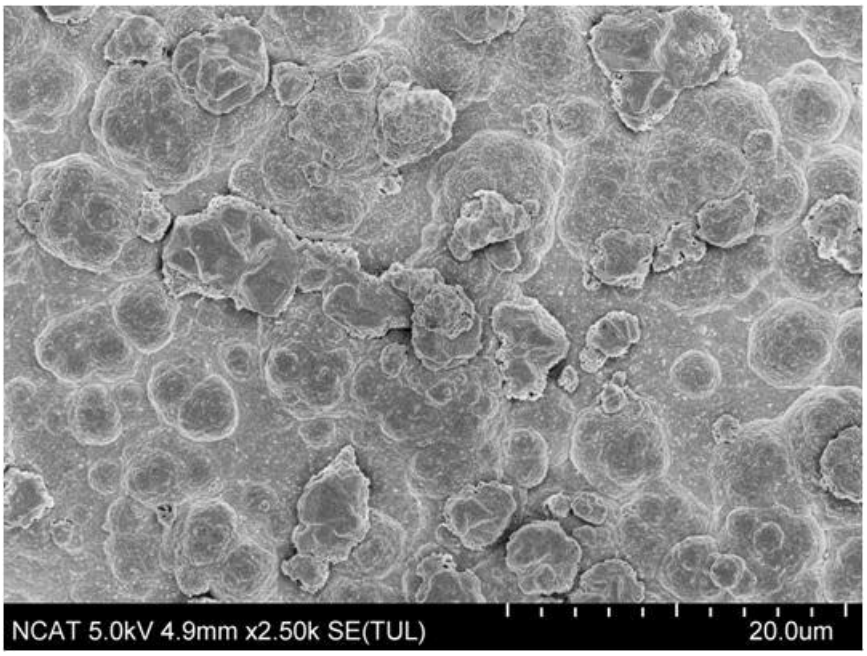

(a) Pd-Ag at 2.5 K (5 kV)

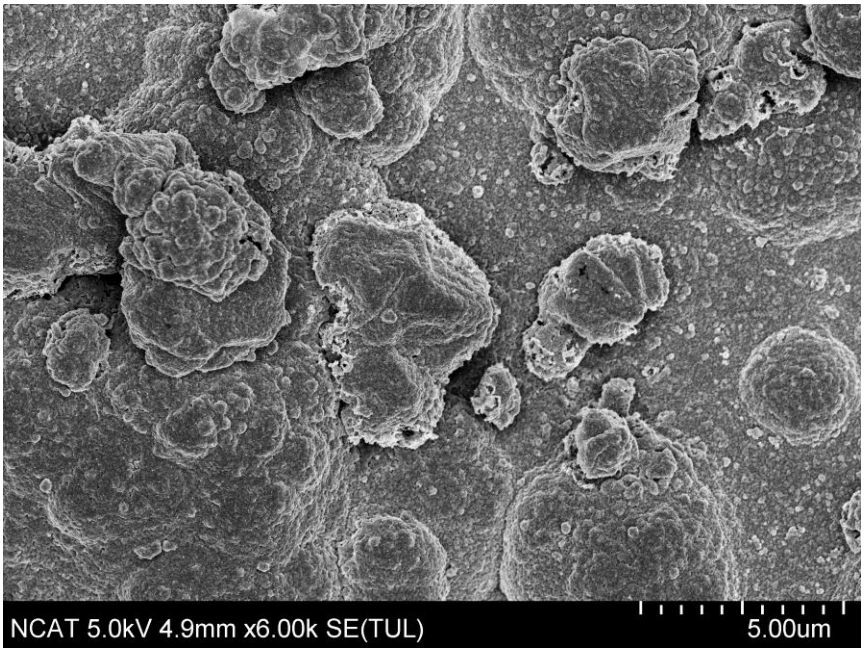

(b) Pd-Ag at 3 K (5 kV)

Figure 12. SEM images of Pd-Ag membrane fabricated by SIEP using 4 CMC and 0.3 CMC of DTAB in Pd- and Ag-bath respectively.

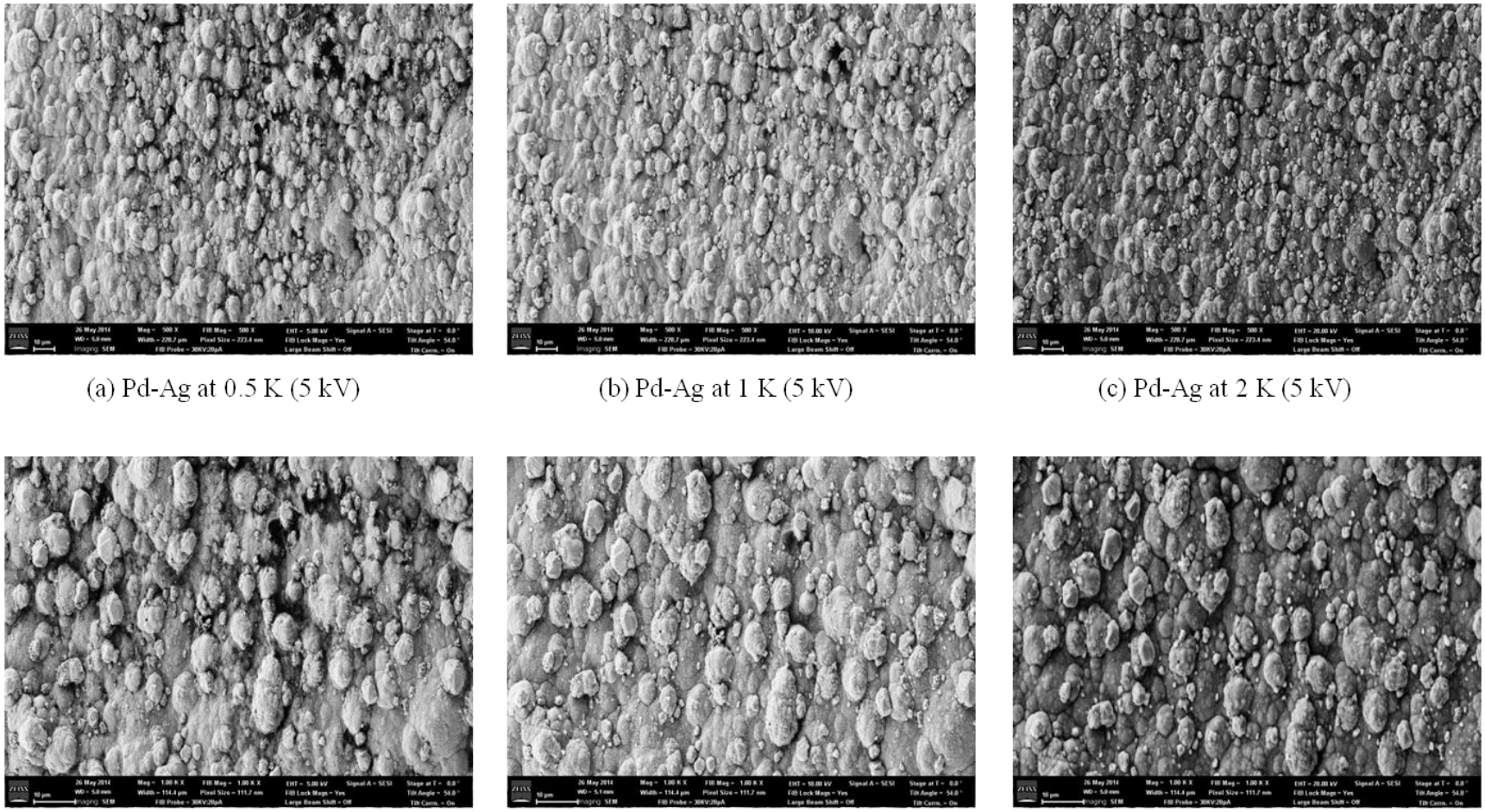

(a) Pd-Ag at 0.5 K (5 kV)

(b) Pd-Ag at 1 K (5 kV)

(c) Pd-Ag at 2 K (5 kV)

(d) Pd-Ag at 0.5 K (10 kV)

(e) Pd-Ag at 1 K (10 kV)

(f) Pd-Ag at 2 K (10 kV)

Figure 13. SEM images of Pd-Ag membrane fabricated by SIEP using 4 CMC and 0.3 CMC of DTAB in Pd- and Ag-bath respectively at different magnifications.

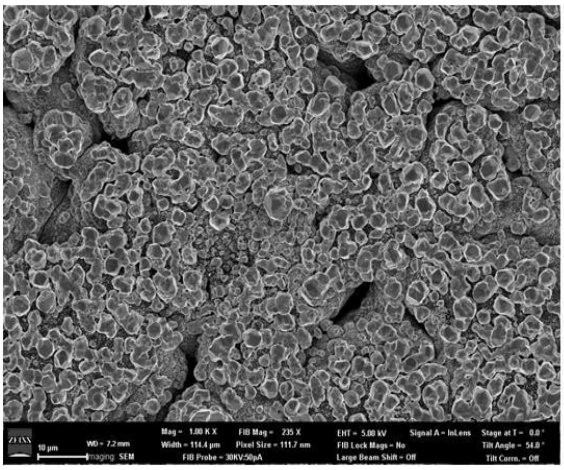

(a) Pd-Ag at 1 K

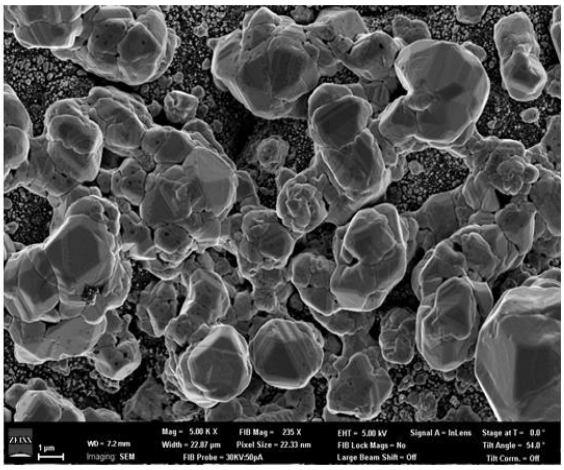

(b) Pd-Ag at 5 K

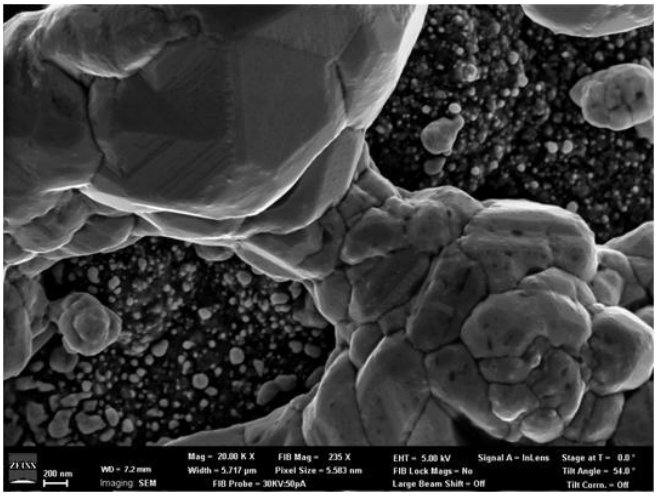

(c) Pd-Ag at 20 K

Figure 14. SEM images of Pd-Ag membrane showing dendritic Ag deposition with 0.3 CMC of DTAB in Ag-bath.

Uniform agglomeration of particle is the key to fabricate dense defect free Pd-Ag membrane. Non-uniform agglomeration leads to larger particle size and results in thicker Pd-Ag composite membrane. In SIEP technique, the particle size can be reduced using surfactant (DTAB) in the plating bath solution. M A Islam [55] reported that the average reduction of Pd grain size was 2 µm in presence of DTAB at 4 CMC while an average particle size was 8 µm when DTAB was absent.

The particle size distribution of reference and present Pd-Ag membranes are depicted in Figures 15 & 16 respectively. Particle size distribution of present Pd-Ag membrane was calculated from the SEM image shown in Figure 14 (a).Present Pd-Ag membrane shows relatively higher percentage of particle sizes between 0.8 µm to 1.2 µm, whereas, reference Pd-Ag membrane shows particle sizes between 1.4 µm to 2.5 µm.

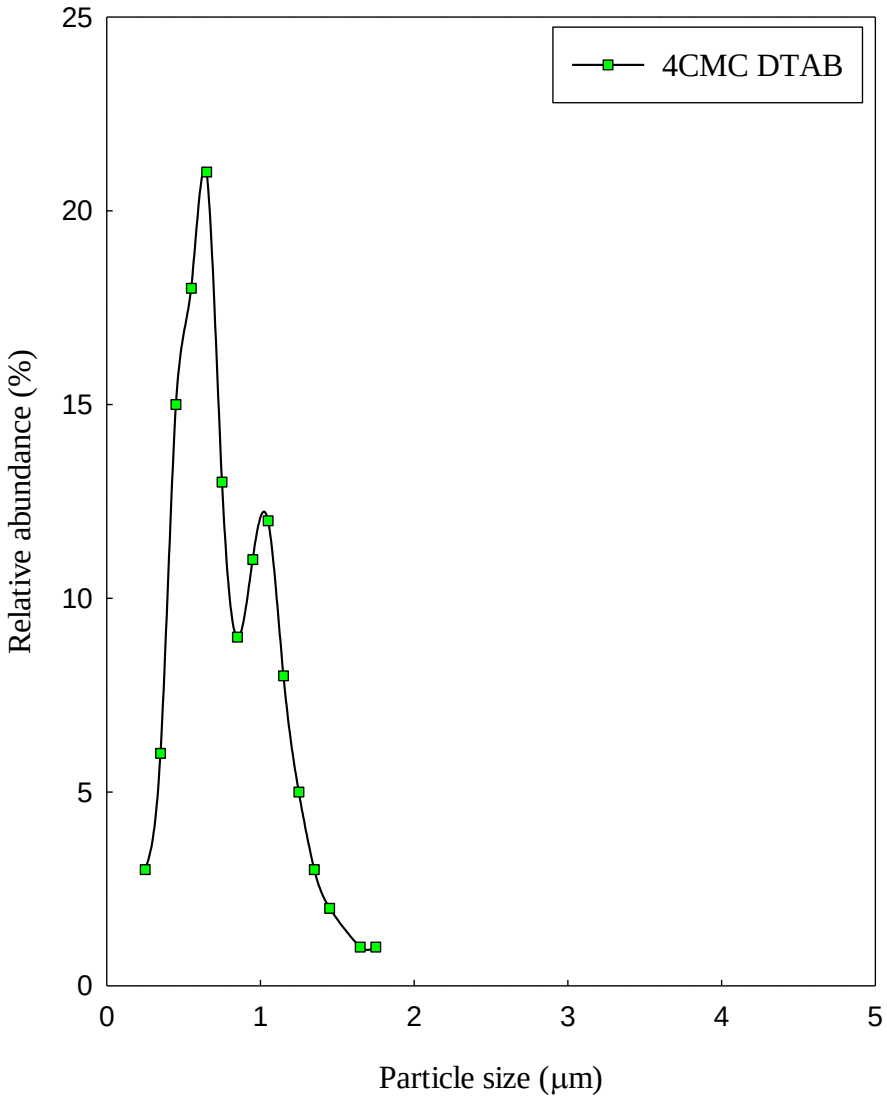

Figure 15. Particle size distribution of Pd-Ag membrane fabricated by SIEP using 4 CMC of DTAB in both Pd- and Ag-bath [16].

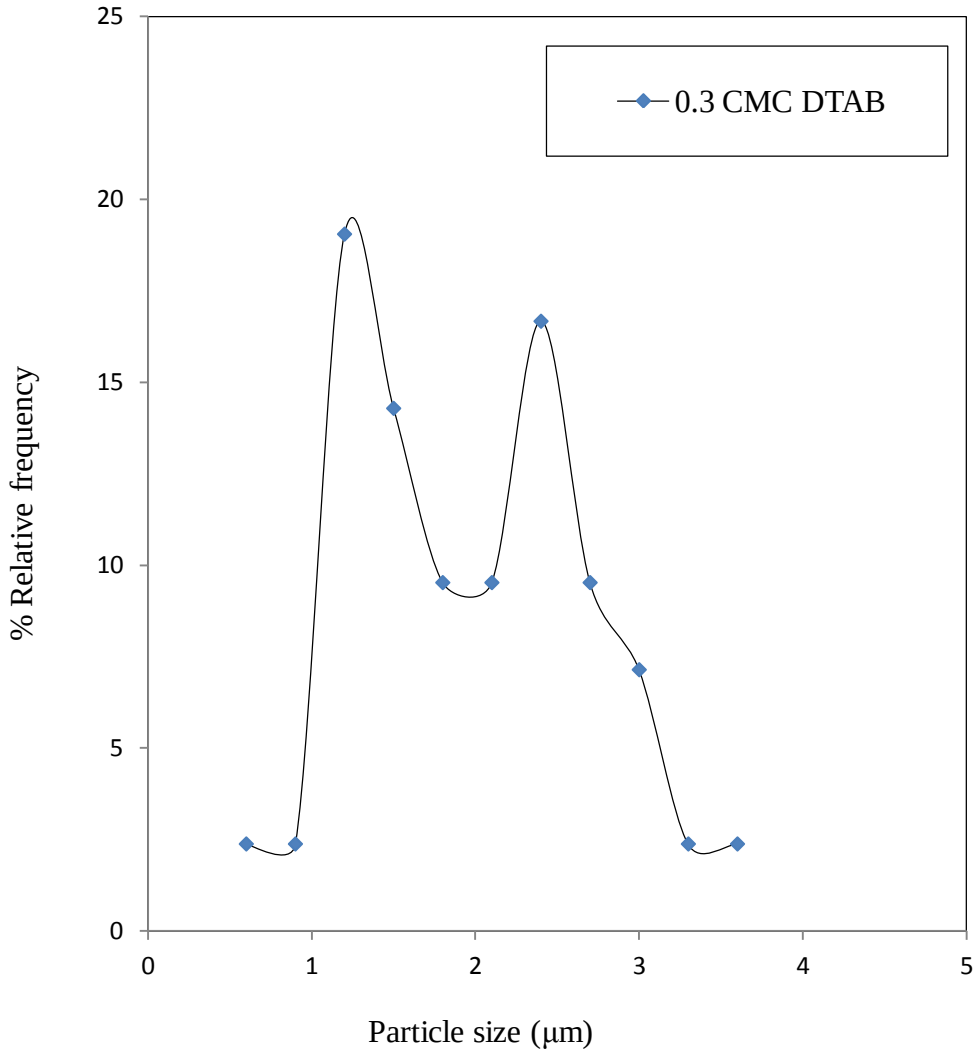

Figure 16. Particle size distribution of Pd-Ag membrane fabricated by SIEP using 4 CMC and 0.3 CMC of DTAB in Pd- and Ag-bath respectively.

The existence of two peaks in Figure 15 and 16 indicate the two different mean size particles for two different deposited metals Pd and Ag which is consistent with the SEM images presented in Figure 14. Pd-Ag membrane fabricated by SIEP using 4 CMC and 0.3 CMC of DTAB in Pd- and Ag-bath respectively shows larger mean particle size than the reference Pd-Ag membrane (4 CMC of DTAB in both Pd- and Ag-bath) mean particle size. This indicates higher CMC of DTAB is more effective to control the particle size and subsequent agglomeration.

However, it was also observed during the experiment that higher CMC of DTAB hinder the Ag deposition and leading to poor surface coverage. So, it is necessary to use different CMC of DTAB in Ag-bath to find out the optimum amount.

A typical XRD pattern for Pd-Ag membrane fabricated by SIEP process is shown in Figure 17. The XRD spectrum show the three major reflection peaks of (111), (200) and (220) planes of pure f.c.c Pd appeared at 2θ = 40.119º, 47.664º and 68.128º, and those of f.c.c Ag phase at 2θ = 38.115º, 44.299º and 64.443º respectively. This implies deposition of polycrystalline structure throughout the surface. Importantly, no reflection was observed for any of the substrate support metal (Fe, Cr, Ni, Mn, &Mo) in the XRD.

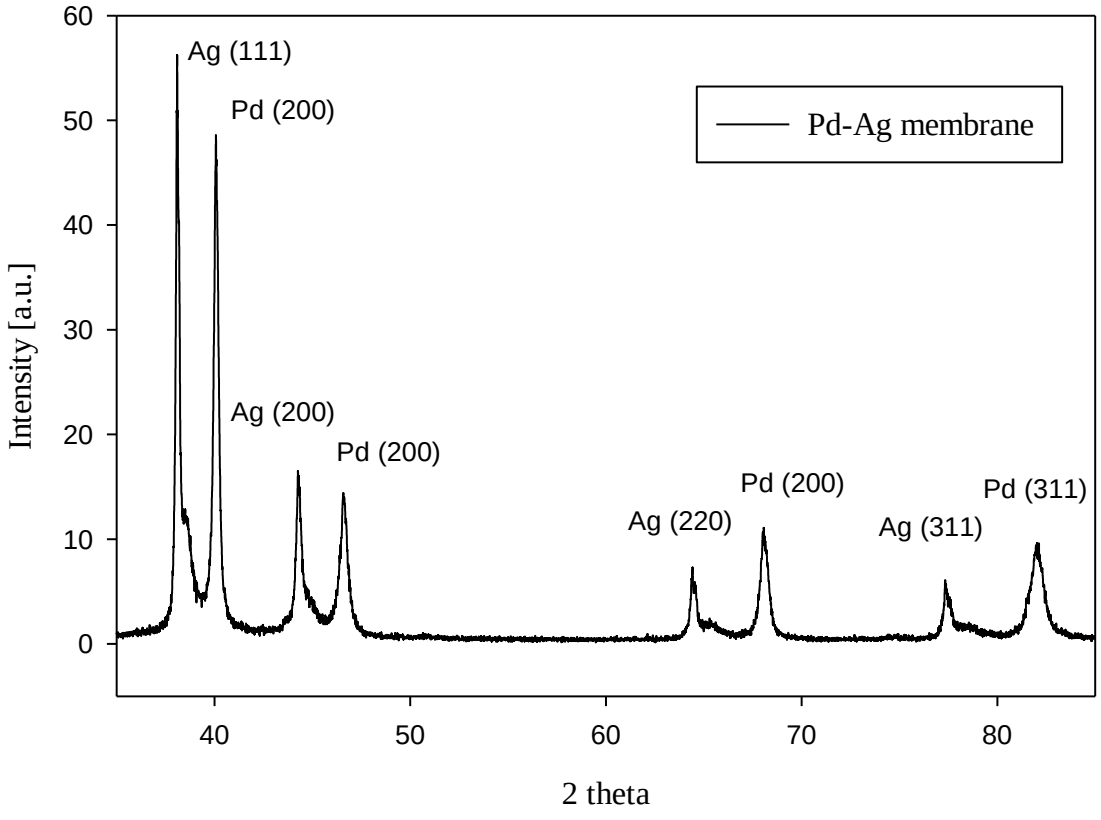

Figure 17. XRD pattern of Pd-Ag film before annealing.

4.2.2 Study of annealing effects on Pd-Ag membranes. Pd and Ag were sequentially deposited by SIEP on the oxide modified support. The composite membranes were annealed at 500 ºC under hydrogen environment for 18 h. The formation of a bulk Pd-Ag alloy was confirmed by XRD analysis. Figure 18 shows the XRD patterns of the type II Pd-Ag membrane before and after annealing. After annealing at 500 ºC, the Ag reflections disappear and new peaks of Pd-Ag membranes appeared at 2θ = 39.92º, 46.44º and 67.76º. All of these peaks are located right between the reflection peaks of Pd (111) and Ag (111), Pd (200) and Ag (200), Pd (220) and Ag (220) respectively that indicates the homogeneous alloy formation of Pd and Ag. Using Brag's law the lattice parameter of Pd-Ag alloy was calculated (Table 6) to be 3.907 Å which was in between the lattice parameters of pure f.c.c Pd (3.889 Å) and pure f.c.c Ag (4.086 Å).

Table 6

XRD Reflection Peaks of Pd-Ag film (type II) Fabricated by SIEP Process

	Bravais lattice	Pd-Ag-film		
		Pd	Ag	Pd-Ag
		(Pre annealed)	(Pre annealed)	(Post annealed)
2-theta	111	40.119	38.11	39.925
	200	46.61	44.31	46.444
	220	68.128	64.429	67.767
	311	82.01	77.392	81.75
d-spacing	111	2.24565	2.35917	2.25628
	200	1.94692	2.0431	1.954
	220	1.37516	1.44469	1.38169
	311	1.17394	1.22204	1.17831
Lattice parameter, a		3.8895	4.0864	3.907
Lattice structure		FCC	FCC	FCC

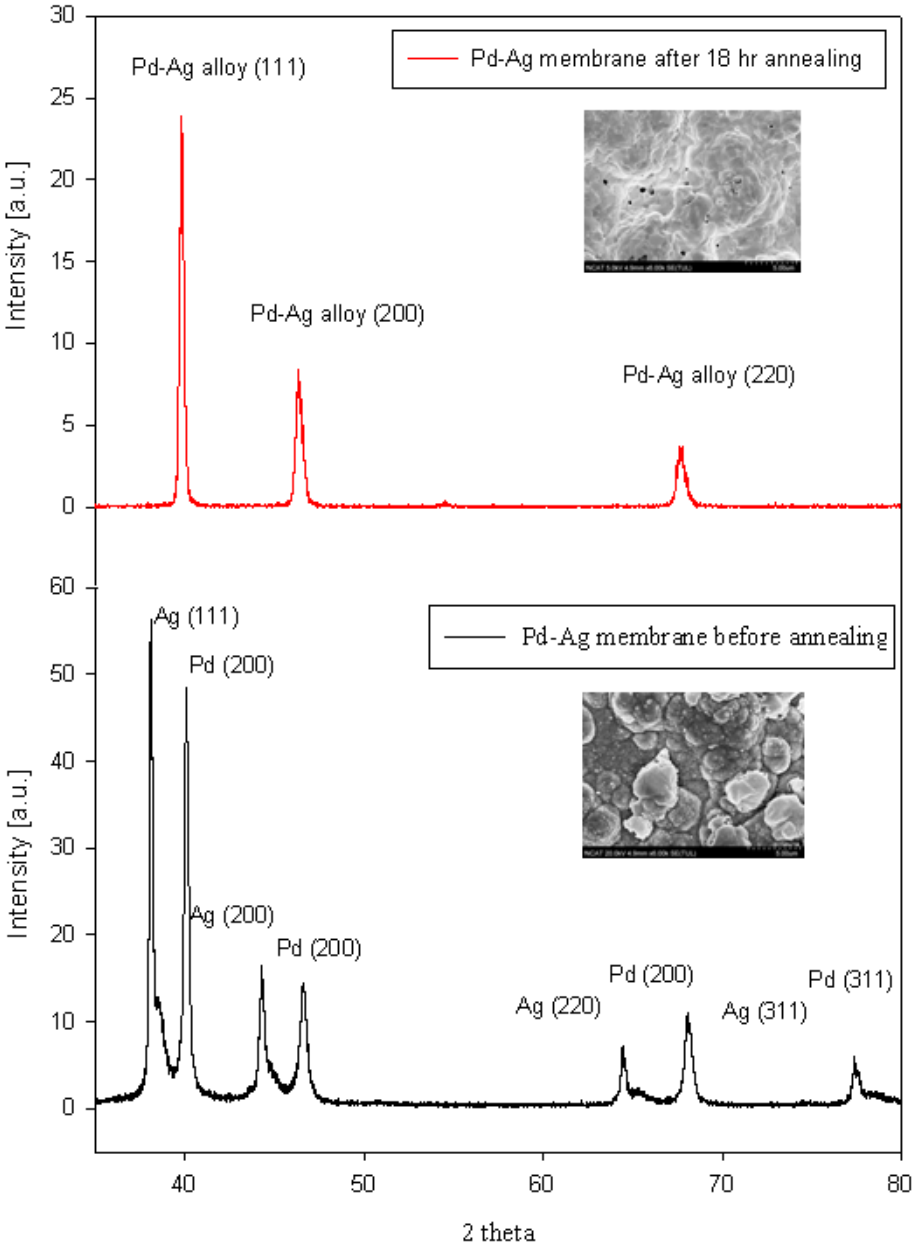

Figure 18. XRD spectra of Pd-Ag film before and after annealing.

Surface elemental analysis was carried out by energy dispersive spectroscopy (EDS) after heat treatment of the membrane. In Figure 19, EDS spectrum show the intense peaks for Pd-Ag membrane. Quantitative EDS elemental analysis of Pd-Ag film shows 20 % (wt) Ag on the top surface of the Pd-Ag barrier film and it may vary along the cross section. As Pd & Ag are placed next to each other in the periodic table, both metals give sharp peaks nearly at the same

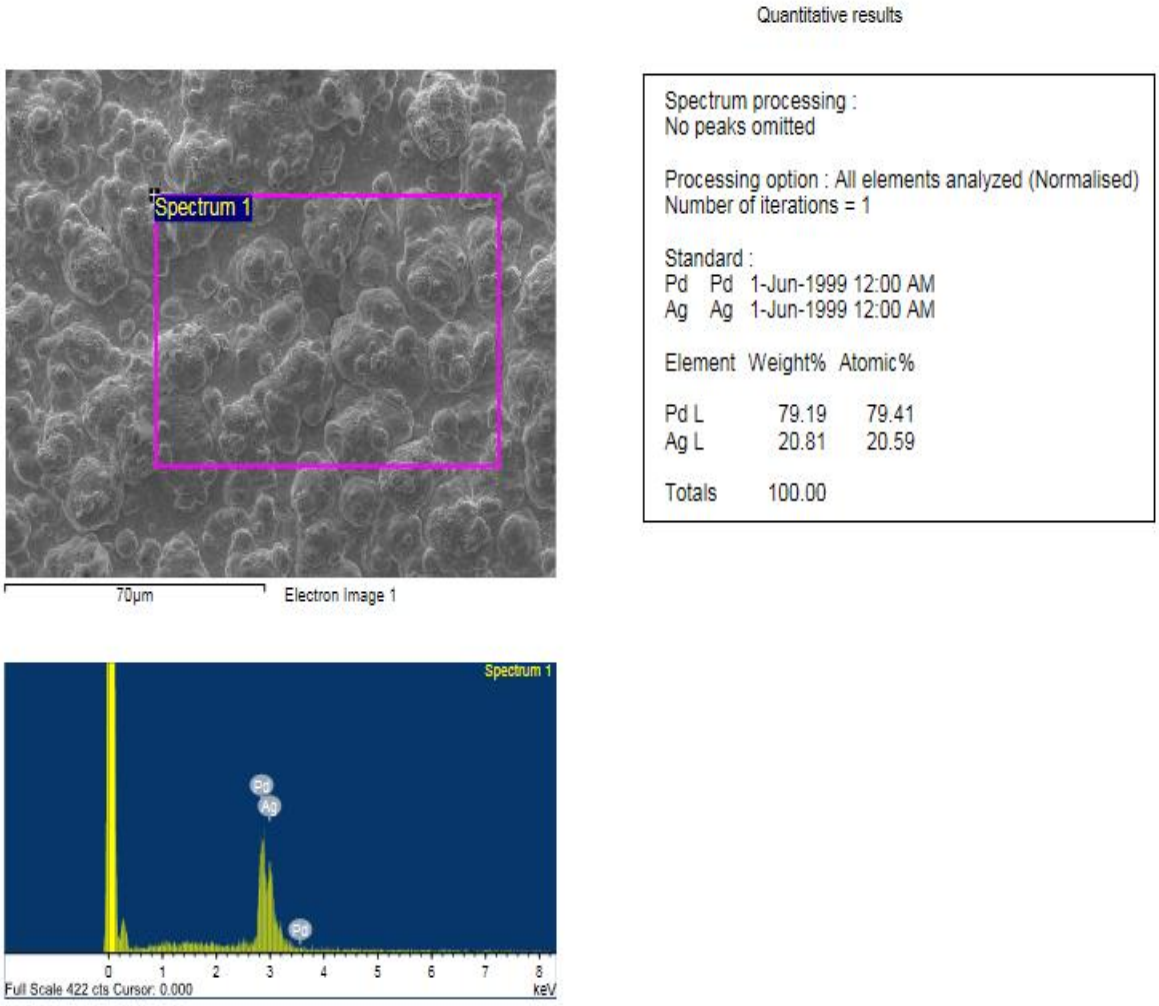

Figure 19. Top surface EDS spectrum of Pd-Ag membrane.

place. No impurities were observed from the EDS spectrum. Figure 20 shows the surface morphology of Pd-Ag membrane fabricated by SIEP using 4 CMC and 0.3 CMC of DTAB in Pd- and Ag- bath respectively after heat treatment at 500 ºC. The Tammann temperature of Ag and Pd are 344 ºC and 640 ºC respectively [61], [62]. As expected, Ag particles diffused into the Pd layers forming homogeneous alloys of larger clusters. From the SEM images, it is clearly observed that the smaller grains agglomerated into larger grains with recognizable boundaries. The agglomerated grain becomes smoother than the un-annealed layer, having morphology of cauliflower.

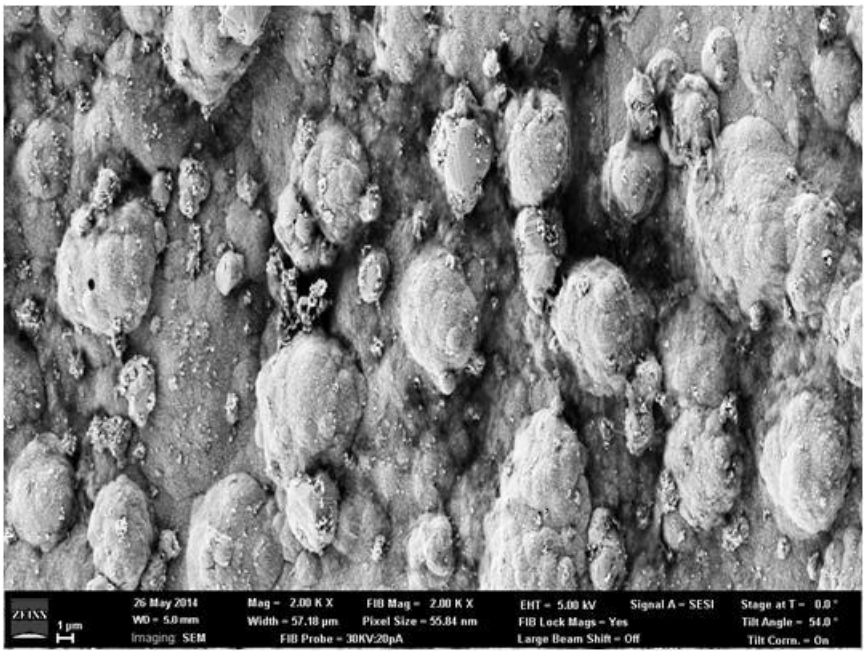

(a) Before annealing

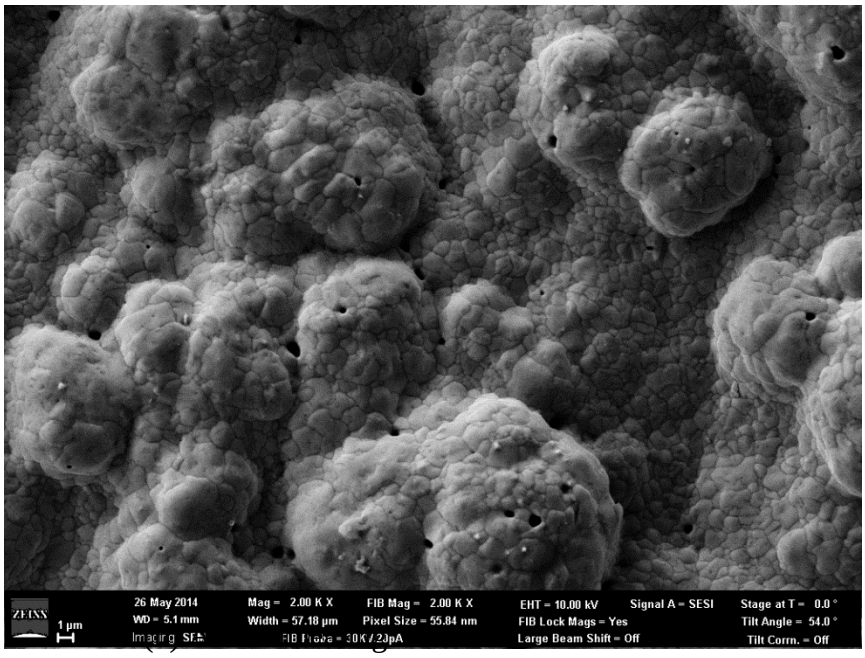

(b) After annealing

Figure 20. SEM images of Pd-Ag membrane showing the effect of heat treatment at 500 ºC.

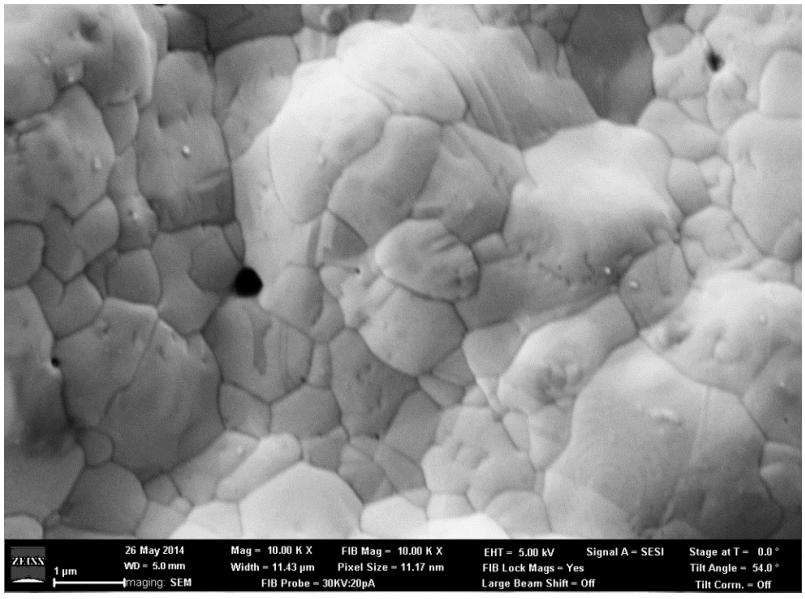

(a) Location 1

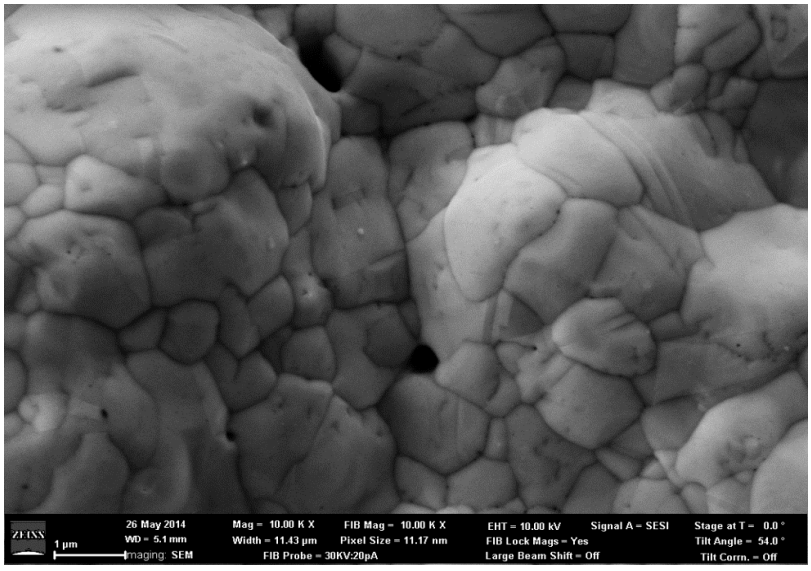

(b) Location 2

Figure 21. SEM images of Pd-Ag membrane after annealing at different location.

From SEM images (Figure 21), pinholes are observed on the top layer of Pd-Ag membrane after annealing. The actual reasons for the pinhole formation are not yet clear. However, Rahman [16] described the possible reasons for the pinhole formation. The oxide layer may form during the drying steps of each sequential deposition. During annealing, oxide layer is

reduced by hydrogen and forms pinholes in the Pd-film. The connectivity of top layer pinholes to the substrate also studied and found no substrate element along the pore depth. The pinholes channels were found only few micrometers from the top layer.

4.3 Hydrogen Permeation Studies of Pd-Ag Membranes

Hydrogen permeation tests were studied using pure hydrogen at temperature of 250-550 ºC and pressure differences across the membrane of 20-100 psi. Simultaneously, nitrogen leak tests were also carried out with same hydrogen permeation test condition. The permeate side pressure was always kept at ambient condition during hydrogen permeation test and the fluxes of pure hydrogen and pure nitrogen were measured as a function of pressure difference across the membrane. During permeation tests, membranes were always heated up to 250 ºC under nitrogen gas environment in the beginning and purged thoroughly with nitrogen before cooling down to ambient temperature. In this study, hydrogen permeability tests and nitrogen leak test were carried out at pressure interval of 20 psi in the range of 20-100 psi at four constant temperatures 250 ºC, 350 ºC, 450 ºC, and 550 ºC. In the following section Pd-Ag membrane with oxide layer was compared with Pd-Ag membrane without oxide layer. All the data for Pd-Ag membrane without oxide layer were taken from the previous work [16]. The thicknesses of Pd-Ag film on MPSS support for Pd-Ag membranes with and without oxide layer were found to be 12.06 μm and 12.54 μm respectively. Thickness was measured based on the gravimetric method. Leak test was carried out by helium gas before and after the annealing of membrane. Helium flow through the Pd-Ag membrane before and after the heat treatment was almost zero and 0.2 ml/min, respectively. The fluxes were measured by water column displacement method. Hydrogen permeances for the Pd-Ag membranes with and without oxide layer were found to be 25.83 m^3/m^2-h and 18.55 m^3/m^2-h at 275 kPa and 450 ºC respectively. The selectivity of hydrogen with

respect to nitrogen for Pd-Ag membrane with and without oxide layer was found to be 500 and 212, respectively. This suggests that Pd-Ag membrane with an oxide layer perform better than Pd-Ag in terms of permeability and selectivity at the specified condition.

The transport of hydrogen through dense Pd or Pd alloy film involves many steps. The hydrogen permeation through the dense Pd based membrane follows the solution diffusion mechanism. The hydrogen flux through dense Pd-Ag membrane was calculated using equation (5).

$$N_H = \frac{Q_H}{t}(P_f^n - P_p^n) \quad (5)$$

where Q_H is the hydrogen permeability (a product of solubility and diffusivity), t is the membrane thickness, and P_f and P_p are the partial pressures of hydrogen on the high and low pressure sides, respectively.

The calculated permeability data for Pd-Ag membrane without and with oxide layer are presented in Figures 22 and 23 respectively as a function of pressure difference (P_f - P_p). The lines show an excellent fit with a power index, n = 0.82 and 85. The power index is higher than the Sievert's law index (n = 0.5). Both figures show that hydrogen flux increases with the pressure drop across the membrane at a constant temperature and hydrogen flux increases with the temperature at a constant pressure drop. Both of the membrane had almost the same thickness and as well Ag % (wt). If hydrogen diffusion becomes the rate determining step for hydrogen permeation, then hydrogen concentration becomes proportional to the square root of hydrogen pressure in accordance with Sievert's law. However, for thick dense metallic membranes n values higher than 05 have been reported [63]. It is expected that the pressure exponent will be higher than 0.5 for the thin metallic membrane and pressure exponent will be close to 1. When surface reaction becomes the rate limiting step, it is believed that hydrogen diffusivity may

become dependent on the concentration of dissolved hydrogen which may contribute to *n* values greater than 0.5 [64],[65].

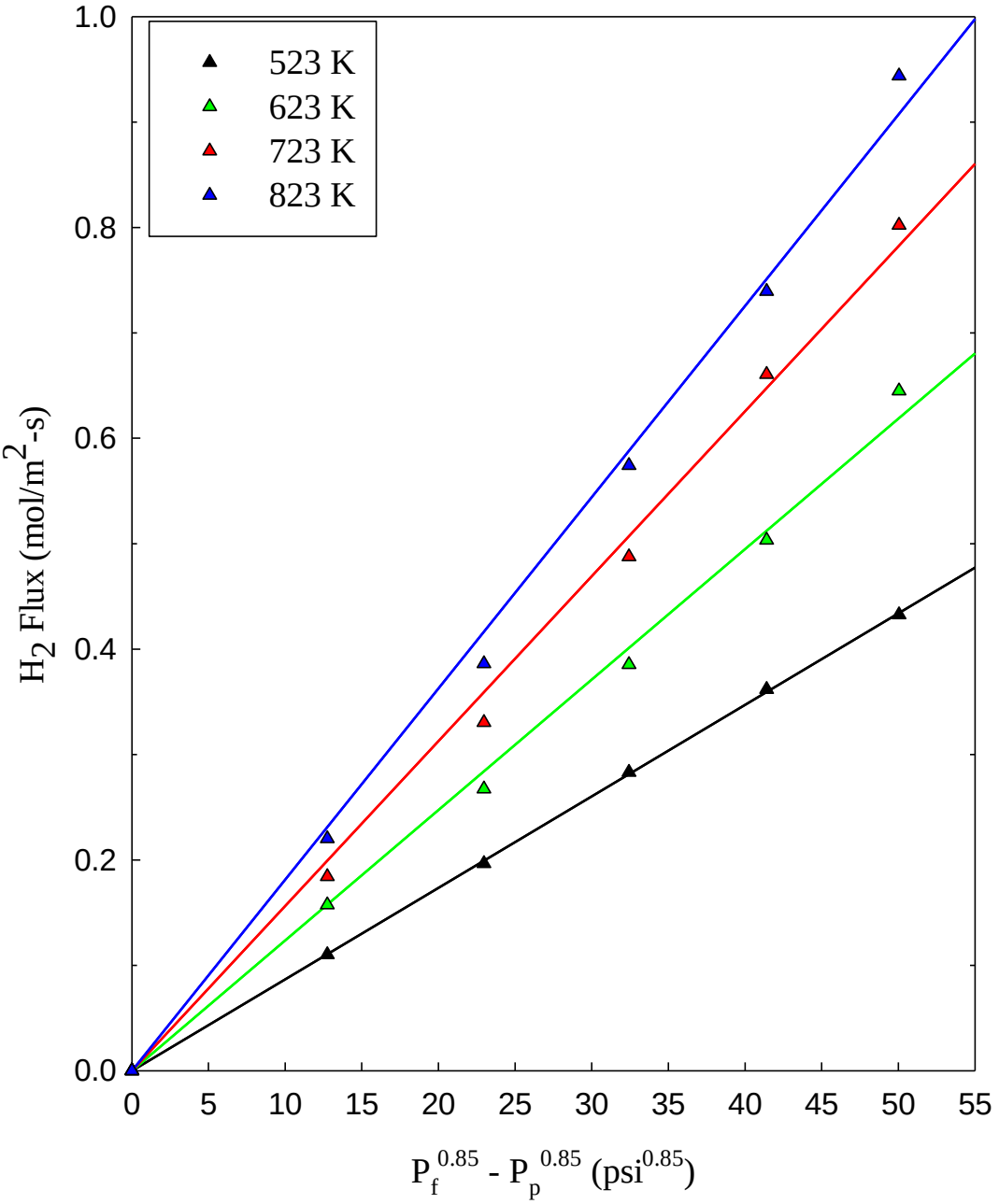

Figure 22. H_2 flux in Pd-Ag membrane without oxide layer at different temperatures [16].

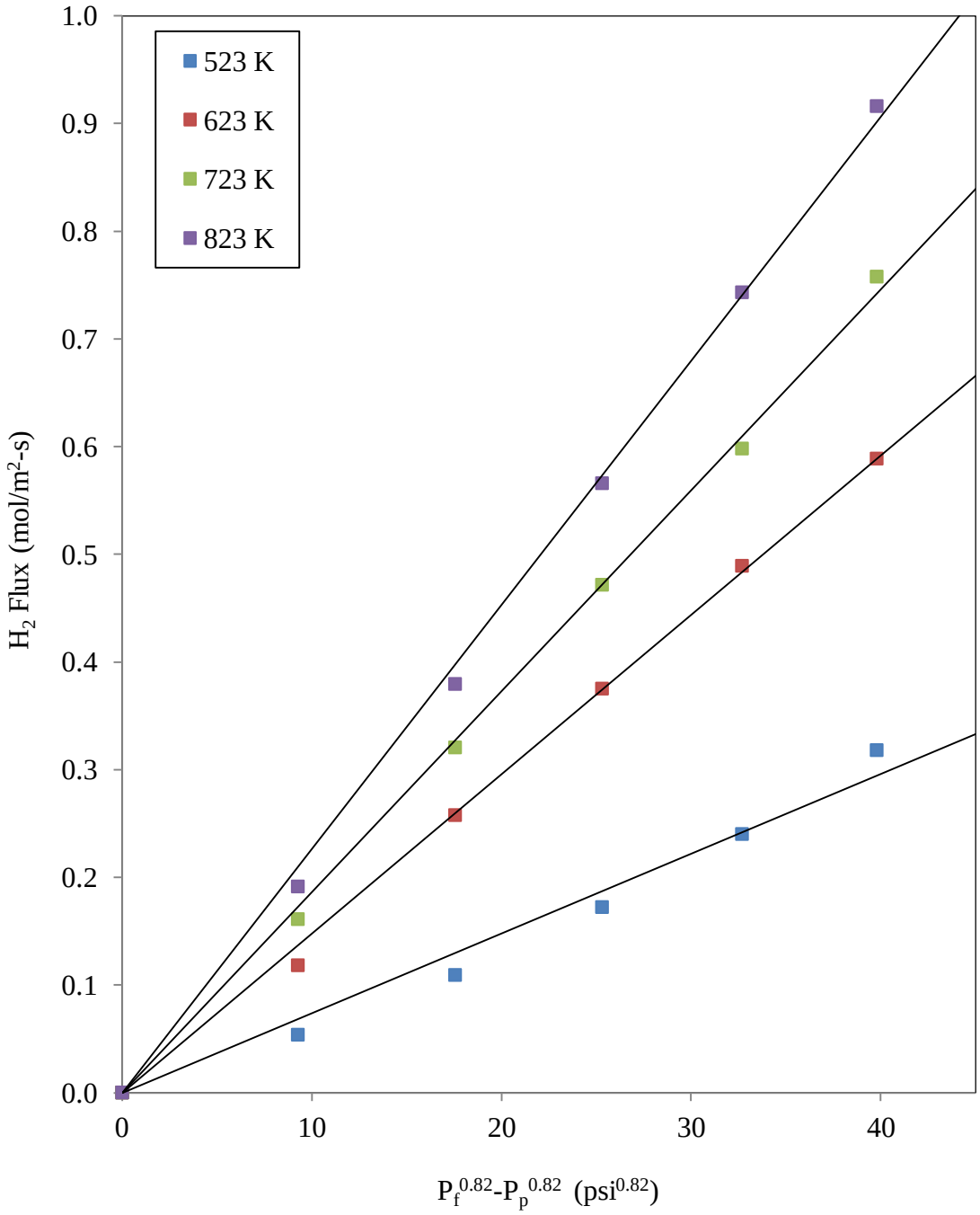

Figure 23. H_2 flux in Pd-Ag membrane with oxide layer at different temperatures.

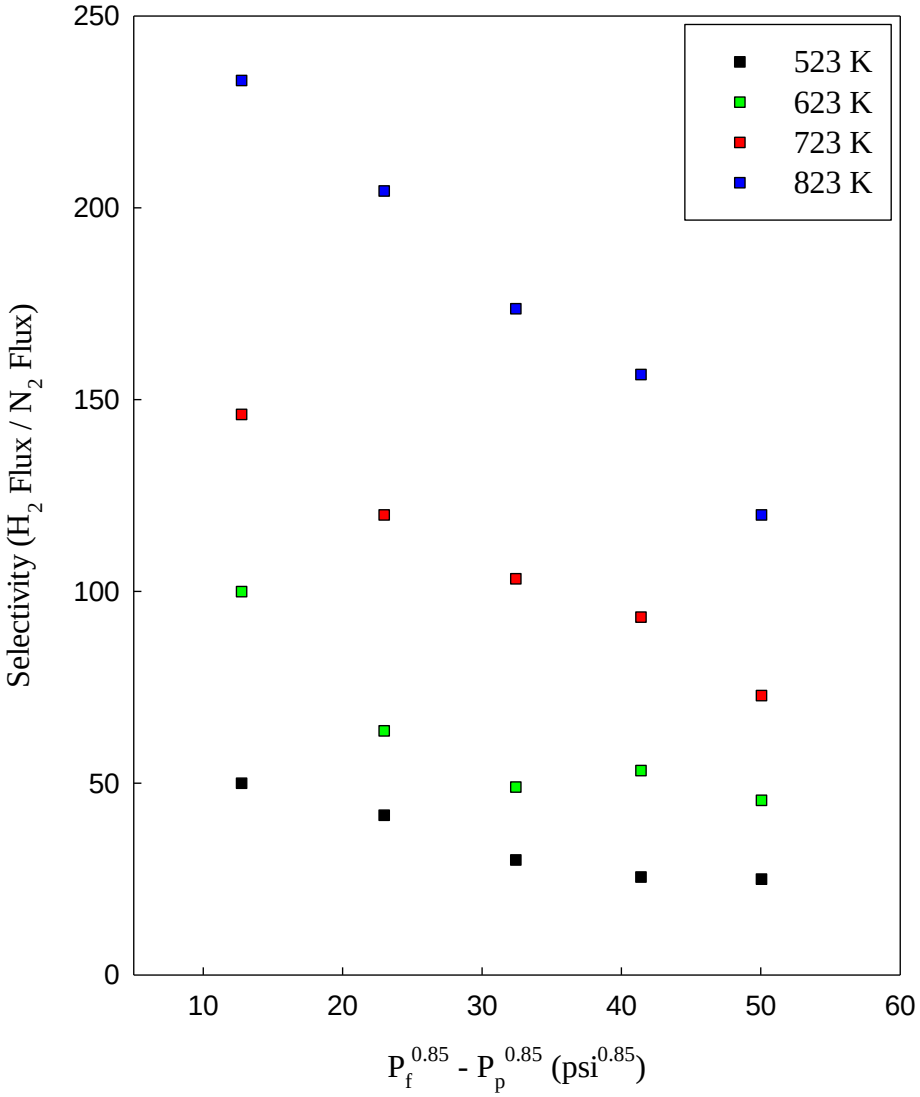

Figure 24. H_2 to N_2 selectivity in Pd-Ag membrane without oxide layer at different temperatures [16].

Leakage of hydrogen through defects in the metal film or membrane seals and resistance of the MPSS membrane support or oxide layer may also slightly increase the index value. However, despite all possible reasons, the deviation of index value from the Sievert's law cannot be concluded clearly [66]. Figures 24 and 25 have shown the hydrogen selectivity plot of Pd-Ag membrane without and with oxide layer, respectively.

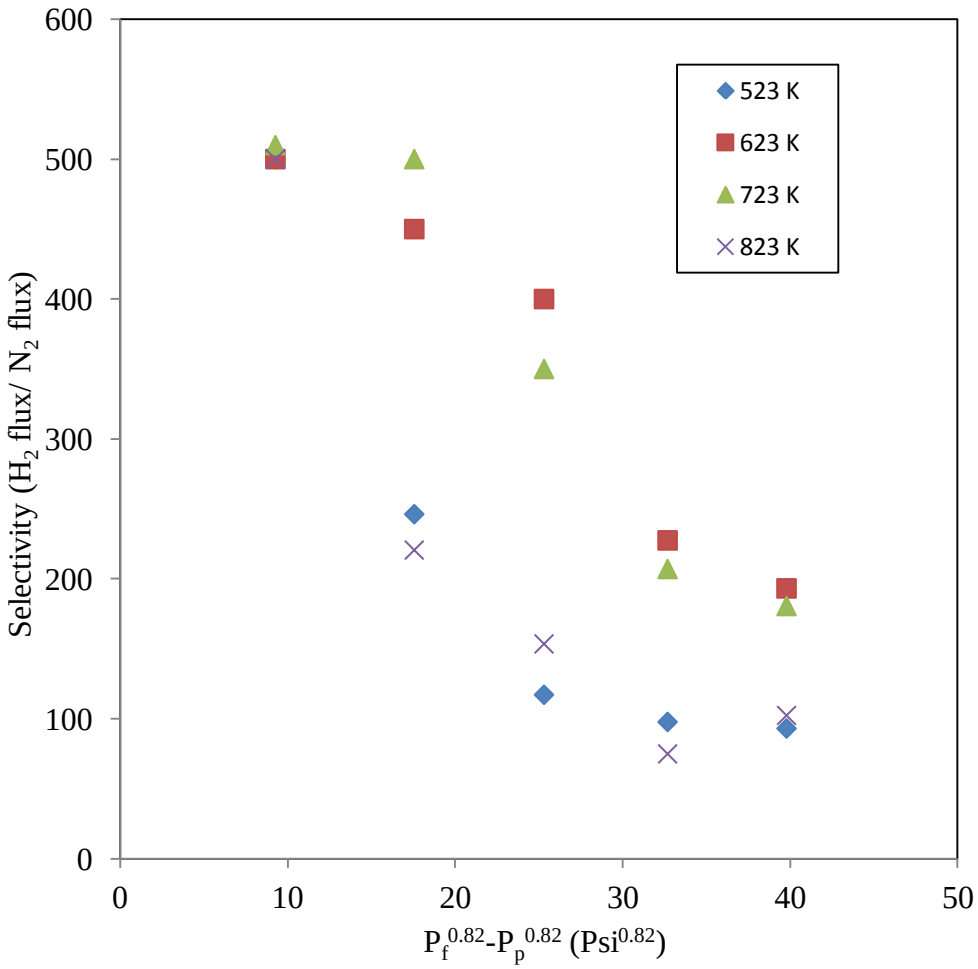

Figure 25. H_2 to N_2 selectivity in Pd-Ag membrane with oxide layer at different temperatures.

The hydrogen selectivity was calculated by the ratio of hydrogen flux versus the nitrogen flux under identical conditions of temperature and pressure. In this work, the maximum temperature and minimum pressure drop were 550 ºC and 20 psi, respectively. The selectivity at 550 ºC and 20 psi was found to be 500 for Pd-Ag with oxide layer. The Pd-Ag membrane with an oxide layer shows significant improvement in terms of selectivity. It is notable that the selectivity of Pd-Ag at 550 ºC drops significantly with pressure difference. The oxide layer was formed at 500 ºC. It may be reduced at 550 ºC under hydrogen environment and create holes in the membrane. As a result, selectivity drops sharply at higher temperature.

To illustrate the intrinsic membrane behavior of the SIEP Pd membranes, the calculated permeability coefficients Q_H at four temperatures are shown in Figures 26 and 27 as an Arrhenius plot (Q_H vs. 1/T). It gives an excellent fit to the Arrhenius equation which can be written as

$$Q_H = Q_{Ho} \exp\left(-E / RT\right) \quad (6)$$

where Q_{Ho} is the reference permeance, E is the activation energy, T is the absolute temperature and R is the universal gas constant.

The calculated activation energy of Pd-Ag with oxide layer were found 10.34 KJ/mol. The measured activation energy are within the normal range of the reported values (7-20 KJ/mol [9]). Table 7 shows that activation energy of Pd and Pd alloy (Pd-Ag and Pd-Cu) membranes fabricated by SIEP. Based on the data in Table 7, the calculated activation energy for Pd-Ag membrane without oxide layer was lower than that for the pure Pd (9.8 KJ/mol). The higher activation energy of Pd-Ag membrane than pure Pd could be the effect of the addition of Ag into the Pd [67].

Table 7

Comparison of Activation Energy of Pd and Pd-alloy Composite Membranes

Name of Membrane	Fabrication Process	Membrane Thickness(μm)	Activation Energy (E), (KJ/mol)	Ref.
Pd/PSS	SIEP	8.5	9.8	[16]
Pd/Ag/PSS	SIEP	12.54	8.7	[16]
Pd/Cu/PSS	SIEP	13.34	8.6	[57]
Pd/Ag/PSS (Oxide layer)	SIEP	12.06	10.3	This work

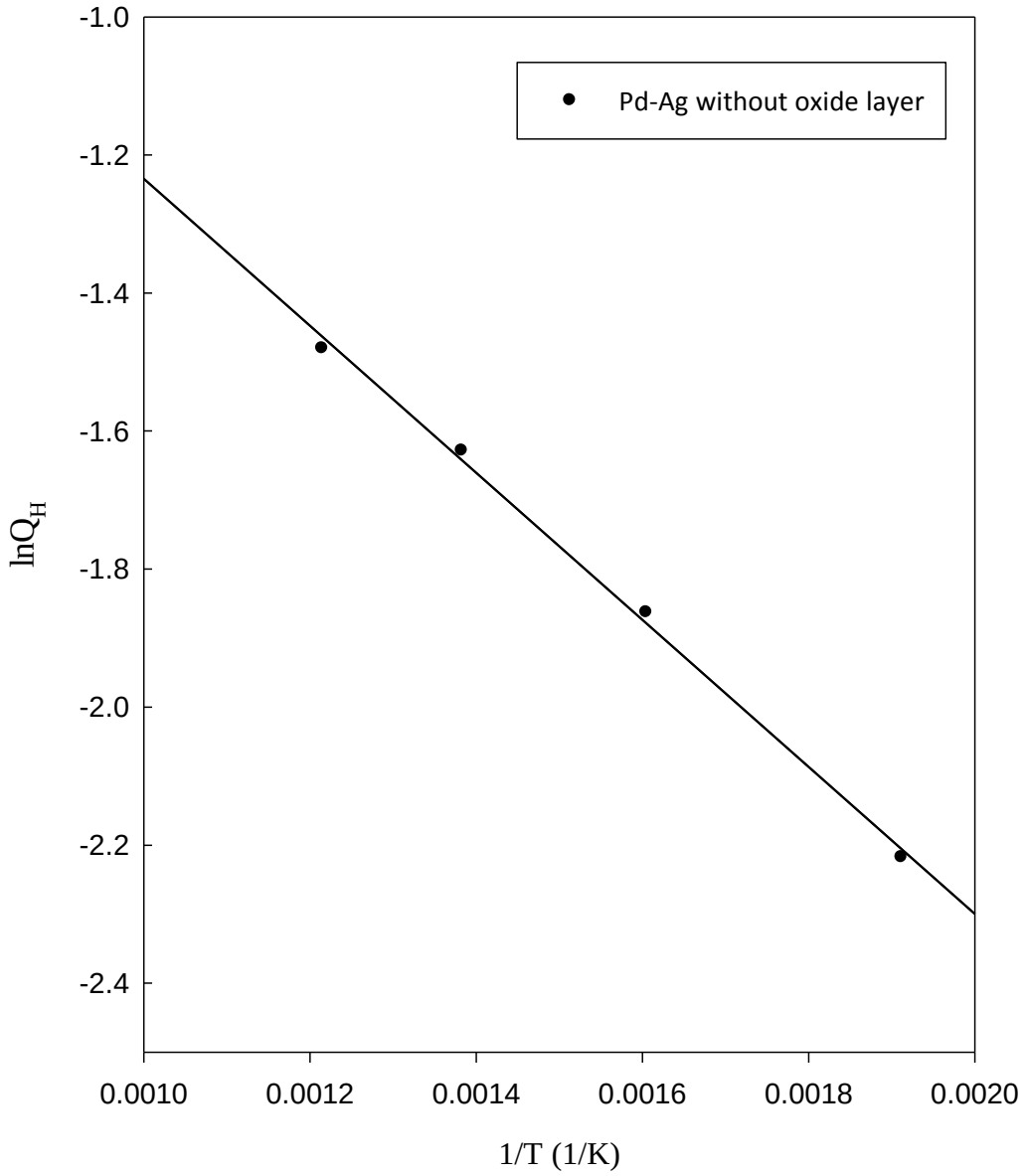

Figure 26. Arrhenius plot of H_2-permeability coefficients of Pd-Ag membrane without oxide layer [16].

The activation energy of H_2 permeability through Pd-Ag membrane depends on two factors: a) diffusion of H-atom, and b) change in enthalpy due to H-atoms solubility [23]. The addition of Ag up to 20-30% (wt) in Pd increased the activation energy of H-atoms diffusion and decreased the change in enthalpy for H-atoms solubility in Pd. The net effect is the decrease in

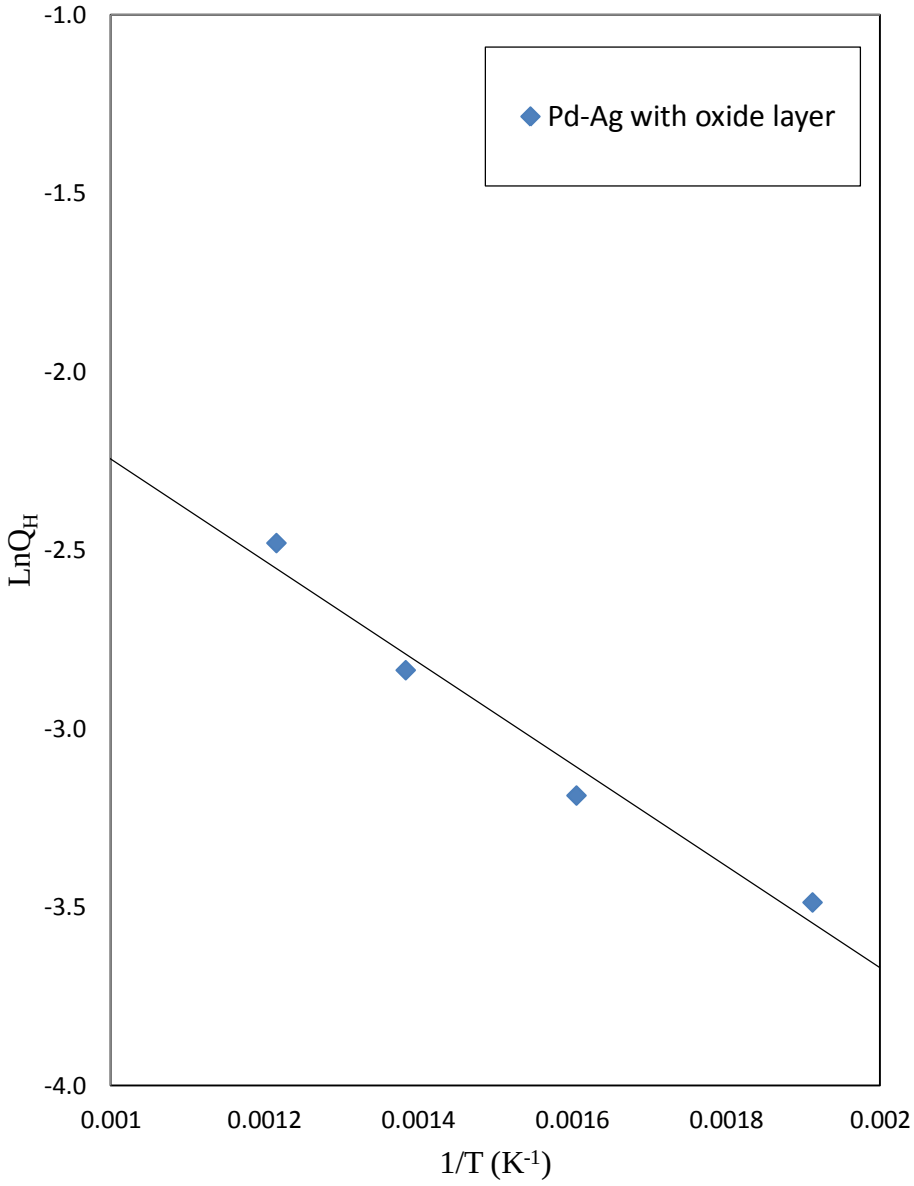

Figure 27. Arrhenius plot of H_2-permeability coefficients of Pd-Ag membrane with oxide layer.

the activation energy of H_2 permeability [23]. The weight percentages of Ag in Pd-Ag membrane with and without oxide layer were 20% and 23%, respectively. Therefore, the activation energy of Pd-Ag membrane without oxide layer was lower than that of the Pd-Ag membrane with oxide layer.

CHAPTER 5

Conclusion and Future Research

5.1 Conclusion

Using SIEP technique, membranes were fabricated by sequential deposition of Pd-Ag films onto oxidized MPSS substrate for hydrogen separation. The oxide layer was formed at 500 ºC in stagnant air prior to metal deposition. The oxide layer did not block the pore of MPSS substrate, but, it significantly reduced the helium flow. In this work, 0.3 CMC of DTAB was used in the Ag-bath to study the effect of surfactant on microstructure from deposition. It was found that the agglomerated particles size with 0.3 CMC of DTAB in Ag-bath were larger than the agglomerated particles size with 4 CMC of DTAB. But, both the membranes showed similar surface morphology and grain agglomeration. Membranes were annealed at 500 ºC and 15 psi under hydrogen environment. The alloy formation of Pd and Ag was confirmed by XRD studies. Membranes were tested for H_2 permeability at a temperature and pressure ranges of 250-550 ºC and 20-100 psi respectively. The performance of the Pd-Ag membrane with oxide layer was changed significantly in comparison to the membrane without oxide layer. Higher permeability and selectivity with respect to N_2 were observed for the Pd-Ag membrane with oxide layer. Film thickness and metal composition were found almost similar for both membranes. Therefore, it can be concluded that addition of oxide layer in Pd-Ag membrane fabricated by SIEP increases the permeability and selectivity of H_2.

5.2 Future Recommendations

The use of surfactant in the electroless plating bath reduces the size of agglomerated particle size which is essential to fabricate dense, thin, and defect free Pd-Ag membrane. But, it is unknown how surfactant works in the electroless plating. It is also necessary to tune the

surfactant concentration for electroless plating bath. Because, lower concentration of surfactant leads larger grain particle, and higher concentration reduces the plating rate as well as poor deposited surface coverage. For further development of Pd-Ag membrane, the following works need to be done:

1. Study of deposited film microstructure by using different CMC of DTAB in Ag-bath. It will help to find out the optimum concentration of DTAB, which will facilitate the formation of smaller grain size with higher plating rate. Intermediate SEM, EDS, and AFM analysis of deposited film will be helpful for this morphological study.
2. For the technical viability, it is required to test the long term performance of Pd-Ag membranes fabricated by SIEP. It was found in the previous work that pure Pd membrane with oxide layer performed 408 h with good H_2 permeability and infinite N_2 selectivity under thermal cycling condition of 300-450 ºC [56]. So, it is expected that with oxide layer the Pd-Ag membrane will show better performance for long period.
3. Fundamental studies of reaction bath kinetics in SIEP technique are essential to understand the role of surfactant. From the kinetic study, it will be easier to select the optimum amount of surfactant for a particular reaction.
4. Finally, demonstration of fabricated Pd-Ag membrane by SIEP as a reactor-separator unit for simultaneous H_2 production and separation

References

1. Urbaniec, K., et al., *Hydrogen for a sustainable global economy.* Journal of Cleaner Production, 2010. **18, Supplement 1**(0): p. S1-S3.
2. Edwards, P.P., V.L. Kuznetsov, and W.I.F. David, *Hydrogen Energy.* Philosophical Transactions: Mathematical, Physical and Engineering Sciences, 2007. **365**(1853): p. 1043-1056.
3. Joseck, F. *Current U.S. Hydrogen Production*. 2012 [cited 2014 June 5]; Available from: http://www.hydrogen.energy.gov/pdfs/12014_current_us_hydrogen_production.pdf.
4. Chaubey, R., et al., *A review on development of industrial processes and emerging techniques for production of hydrogen from renewable and sustainable sources.* Renewable and Sustainable Energy Reviews, 2013. **23**(0): p. 443-462.
5. Adhikari, S. and S. Fernando, *Hydrogen Membrane Separation Techniques.* Industrial & Engineering Chemistry Research, 2006. **45**(3): p. 875-881.
6. Paglieri, S.N. and J.D. Way, *Innovations in Palladium Membrane Research.* Separation & Purification Reviews, 2002. **31**(1): p. 1-169.
7. Ing. Ste&en Wieland, I.T.M., Ing. A. Lammb, *Membrane reactors for hydrogen production.* Chemical Engineering Science, 2002. **57**: p. 1571-1576.
8. Nam, S.-E. and K.-H. Lee, *Hydrogen separation by Pd alloy composite membranes: Introduction of diffusion barrier.* Journal of Membrane Science, 2001. **192**(Compendex): p. 177-185.
9. Xie, D., et al., *Hydrogen permeability of Pd–Ag membrane modules with porous stainless steel substrates.* International Journal of Hydrogen Energy, 2011. **36**(1): p. 1014-1026.

10. Brodowsky, H., *The Palladium Hydrogen System. Von F. A. Lewis, Academic Press, London-New York 1967. 1. Aufl., XII, 178 S., zahlr. Abb., geb. 45 s.* Angewandte Chemie, 1968. **80**(12): p. 498-498.

11. Yun, S. and S. Ted Oyama, *Correlations in palladium membranes for hydrogen separation: A review.* Journal of Membrane Science, 2011. **375**(1–2): p. 28-45.

12. Cheng, Y.S. and K.L. Yeung, *Palladium–silver composite membranes by electroless plating technique.* Journal of Membrane Science, 1999. **158**(1–2): p. 127-141.

13. Fort, D., J.P.G. Farr, and I.R. Harris, *A comparison of palladium-silver and palladium-yttrium alloys as hydrogen separation membranes.* Journal of the Less Common Metals, 1975. **39**(2): p. 293-308.

14. MA, Y.H., I.P. Mardilovich, and E.E. Engwall, *Thin Composite Palladium and Palladium/Alloy Membranes for Hydrogen Separation.* Annals of the New York Academy of Sciences, 2003. **984**(Advanced Membrane Technology): p. 346-360.

15. Ilias, S. and M.A. Islam, *Methods of preparing thin films by electroless plating*, U.S. Patent, Editor 2010: United States.

16. Rahman, M.M., *Fabrication of Pd and Pd-Ag Membranes by Surfactant Induced Electroless Plating (SIEP)*, in *Chemical and Bio-engineering*, 2010, North Carolina A&T State University: Greensboro, North Carolina.

17. Holladay, J.D., et al., *An overview of hydrogen production technologies.* Catalysis Today, 2009. **139**(4): p. 244-260.

18. Schoots, K., et al., *Learning curves for hydrogen production technology: An assessment of observed cost reductions.* International Journal of Hydrogen Energy, 2008. **33**(11): p. 2630-2645.

19. Grashoff, G.J., C.E. Pilkington, and C.W. Corti, *The purification of hydrogen.* Platinum Metals Review, 1983. **27**(4): p. 157-169.

20. Koros, W.J. and G.K. Fleming, *Membrane-based gas separation.* Journal of Membrane Science, 1993. **83**(1): p. 1-80.

21. Zhang, X., G. Xiong, and W. Yang, *A modified electroless plating technique for thin dense palladium composite membranes with enhanced stability.* Journal of Membrane Science, 2008. **314**(1–2): p. 226-237.

22. Ward, T.L. and T. Dao, *Model of hydrogen permeation behavior in palladium membranes.* Journal of Membrane Science, 1999. **153**(2): p. 211-231.

23. Holleck, G.L., *Diffusion and solubility of hydrogen in palladium and palladium--silver alloys.* The Journal of Physical Chemistry, 1970. **74**(3): p. 503-511.

24. Lewis, F.A., *The palladium-hydrogen system: Structures near phase transition and critical points.* International Journal of Hydrogen Energy, 1995. **20**(7): p. 587-592.

25. Rodina, A.A., Gurevich, M.A., Doronicheva, N.I. , *The interaction of hydrogen with certain palladium-gold and palladium-silver-gold alloys.* Russ J Phys Chem, 1971. **45**: p. 621–623.

26. Ohira, K., Y. Sakamoto, and T.B. Flanagan, *Thermodynamic properties for solution of hydrogen in Pd-Ag-Ni ternary alloys.* Journal of Alloys and Compounds, 1996. **236**(1–2): p. 42-49.

27. Rogers, H.C., *Hydrogen Embrittlement of Metals: Atomic hydrogen from a variety of sources reduces the ductility of many metals.* Science, 1968. **159**(3819): p. 1057-1064.

28. Kulprathipanja, A., et al., *Pd and Pd–Cu membranes: inhibition of H2 permeation by H2S.* Journal of Membrane Science, 2005. **254**(1–2): p. 49-62.

29. Pomerantz, N. and Y.H. Ma, *Novel method for producing high H2 permeability Pd membranes with a thin layer of the sulfur tolerant Pd/Cu fcc phase.* Journal of Membrane Science, 2011. **370**(1–2): p. 97-108.

30. L, M.D., *Method for hydrogen separation and purification*, 1969, Google Patents.

31. Massalski, T.B., Okamoto, H., Subramanian, P. R., Kacprzak, L., in *Binary Alloy Phase Diagrams*1990, ASM International. p. 1485.

32. Chen, Y., Atago, T., Mohri, T., *First-principles study for ordering and phase separation in the Fe-Pd system.* Journal of Physics: Condensed Matter, 2002. **14**(8): p. 1903–1913.

33. Bonyuet, D., J. Ochoa, and G. Gonzalez. *Mechanical alloying in the immiscible systems Ag-M (M = Fe, Co, Ni)*. in *Proceedings of the 10th International Symposium on Metastable Mechanically Alloyed and Nanocrystalline Materials (ISMANAM-2002), August 24, 2003 - August 28, 2003*. 2004. Foz do Ifuacu, Brazil: Trans Tech Publications Ltd.

34. Swartzendruber, L.J., *The Ag−Fe (Silver-Iron) system.* Bulletin of Alloy Phase Diagrams 1984. **5**(6): p. 560-564.

35. Schumacher, D., *La diffusion dans les solids: By Y. Adda and J. Philibert, in the Series: Bibliothèque des Sciences et Techniques Nucléaires (Direction F. Perrin), published by Institut National des Sciences et Techniques Nucléaires, Saclay and Press Universitaires de France, Paris, 1966. Two volumes, a total of 1268 pages (in French). Price: Ffr. 106.* Materials science and engineering, 1967. **2**(1): p. 54-54.

36. Huzinec, G.M., R.M. Andrews, and C.P. Bieniasz, *Metal-coated superabrasive material and methods of making the same*, 2008, Google Patents.

37. Xomeritakis, G. and Y.S. Lin, *Fabrication of a thin palladium membrane supported in a porous ceramic substrate by chemical vapor deposition.* Journal of Membrane Science, 1996. **120**(2): p. 261-272.

38. Jun, C.-S. and K.-H. Lee, *Palladium and palladium alloy composite membranes prepared by metal-organic chemical vapor deposition method (cold-wall).* Journal of Membrane Science, 2000. **176**(1): p. 121-130.

39. Mattox, D.M., *Handbook of Physical Vapor Deposition (PVD) Process*, 2010, Elsevier Inc.

40. Nam, S.-E. and K.-H. Lee, *A study on the palladium/nickel composite membrane by vacuum electrodeposition.* Journal of Membrane Science, 2000. **170**(1): p. 91-99.

41. Altinisik, O., M. Dogan, and G. Dogu, *Preparation and characterization of palladium-plated porous glass for hydrogen enrichment.* Catalysis Today, 2005. **105**(3-4).

42. Uemiya, S., et al., *A Palladium/Porous-Glass Composite Membrane for Hydrogen Separation.* Chemistry Letters, 1988. **17**(10): p. 1687-1690.

43. Nam, S.E. and K.H. Lee, *Hydrogen separation by Pd alloy composite membranes: introduction of diffusion barrier.* Journal of Membrane Science, 2001. **192**(1–2): p. 177-185.

44. Shu, J., et al., *Structurally stable composite Pd-Ag alloy membranes: introduction of a diffusion barrier.* Thin Solid Films, 1996. **286**(Copyright 1997, FIZ Karlsruhe): p. 72-9.

45. Nam, S.-E., S.-H. Lee, and K.-H. Lee, *Preparation of a palladium alloy composite membrane supported in a porous stainless steel by vacuum electrodeposition.* Journal of Membrane Science, 1999. **153**(2): p. 163-173.

46. Yepes, D., et al., *Different oxides used as diffusion barriers in composite hydrogen permeable membranes.* Journal of Membrane Science, 2006. **274**(1–2): p. 92-101.

47. Ma, Y.H., Mardilovich, Peter P., She, Ying, *Hydrogen gas-extraction module and method of fabrication*, 2000, Worcester, Polytechnic Institute (Worcester, MA): United States.

48. Wang, D., et al., *Preparation of palladium membrane over porous stainless steel tube modified with zirconium oxide.* Catalysis Today, 2004. **93–95**(0): p. 689-693.

49. Ayturk, M.E., et al., *Synthesis of composite Pd-porous stainless steel (PSS) membranes with a Pd/Ag intermetallic diffusion barrier.* Journal of Membrane Science, 2006. **285**(1-2): p. 385-394.

50. Mallory, G.O.H.J.B., ed. *Electroless Plating - Fundamentals and Applications*. 1990, William Andrew Publishing/Noyes.

51. Ayturk, M.E. and Y.H. Ma, *Electroless Pd and Ag deposition kinetics of the composite Pd and Pd/Ag membranes synthesized from agitated plating baths.* Journal of Membrane Science, 2009. **330**(Compendex): p. 233-245.

52. Rhoda, R.N., A.-M. Madison, *Palladium plating by chemical reduction*, 1959, INT NICKEL CO: United States.

53. Chen, B.H., et al., *Effects of surfactants in an electroless nickel-plating bath on the properties of Ni-P alloy deposits.* Industrial and Engineering Chemistry Research, 2002. **41**(Compendex): p. 2668-2678.

54. Islam, M.A., *The development of improved electroless plating in fabricating Pd-based membrane and membrane reactor application for hydrogen separation*, in *Energy and Environmental Studies*, 2008, North Carolina A & T State University: Greensboro, NC.

55. Islam, M.A. and S. Ilias, *Characterization of Pd-composite membrane fabricated by surfactant induced electroless plating (SIEP): Effect of grain size on hydrogen permeability.* Separation Science and Technology, 2010. **45**(12-13): p. 1886-1893

56. Islam, S., *A Study on Thermal Stabilty of Palladium-Composite Membrane Fabricated by Surfactant Induced Electroless Plating (SIEP)*, in *Chemical & Bioengineering*, 2012, North Carolina A&T State University, Greensboro, North Carolina.

57. Islam, M.S., M.M. Rahman, and S. Ilias, *Characterization of Pd–Cu membranes fabricated by surfactant induced electroless plating (SIEP) for hydrogen separation.* International Journal of Hydrogen Energy, 2012. **37**(4): p. 3477-3490.

58. Ma, Y.H., et al., *Characterization of intermetallic diffusion barrier and alloy formation for Pd/Cu and Pd/Ag porous stainless steel composite membranes.* Industrial and Engineering Chemistry Research, 2004. **43**(Compendex): p. 2936-2945.

59. Mardilovich, P.P., et al., *Defect-free palladium membranes on porous stainless-steel support.* AIChE Journal, 1998. **44**(Compendex): p. 310-322.

60. Akis, B.C., et al., *Effects of the in-situ formation of an intermetallic diffusion barrier layer on the properties of composite Palladium membranes.* ACS Fuel Chem. Div. Preprints, 2003. **48**(1): p. 337.

61. Ma, Y.H., P.P. Mardilovich, and Y. She, *Method for selectively separating hydrogen from hydrogen-producing reactants*, 2000, Google Patents.

62. Shu, J., et al., *Structurally stable composite Pd・Ag alloy membranes: Introduction of a diffusion barrier.* Thin Solid Films, 1996. **286**(1–2): p. 72-79.

63. Guazzone, F., E.E. Engwall, and Y.H. Ma, *Effects of surface activity, defects and mass transfer on hydrogen permeance and n-value in composite palladium-porous stainless steel membranes.* Catalysis Today, 2006. **118**(1–2): p. 24-31.

64. Collins, J.P. and J.D. Way, *Preparation and characterization of a composite palladium-ceramic membrane.* Industrial and Engineering Chemistry Research, 1993. **32**(Compendex): p. 3006-3013.

65. Uemiya, S., et al., *Separation of hydrogen through palladium thin film supported on a porous glass tube.* Journal of Membrane Science, 1991. **56**(3): p. 303-313.

66. Caravella, A., G. Barbieri, and E. Drioli, *Modelling and simulation of hydrogen permeation through supported Pd-alloy membranes with a multicomponent approach.* Chemical Engineering Science, 2008. **63**(8): p. 2149-2160.

67. Ackerman, F.J. and G.J. Koskinas, *Permeation of hydrogen and deuterium through palladium-silver alloys.* Journal of Chemical & Engineering Data, 1972. **17**(1): p. 51-55.